UNCLASSIFIED

AD 414369

DEFENSE DOCUMENTATION CENTER

FOR

SCIENTIFIC AND TECHNICAL INFORMATION

CAMERON STATION, ALEXANDRIA, VIRGINIA

UNCLASSIFIED

63-4-5

Limitations of
Space-Time Harmonics
For Microwave Amplification

by

T. E. Everhart
J. Horowitz

DDC

AUG 26 1963

TISIA D

ELECTRONICS RESEARCH LABORATORY

Electronics Research Laboratory
University of California
Berkeley, California

LIMITATIONS OF SPACE-TIME HARMONICS FOR MICROWAVE AMPLIFICATION

by

T. E. Everhart

J. Horowitz

FOREWORD

i

ACKNOWLEDGMENT

ABSTRACT

The possibility of gain utilizing the interaction between an electromagnetic wave in a smooth wave guide and a space-time harmonic of the slow space-charge wave has been proposed as a method of millimeter-wave amplification. A model is proposed here which satisfies the conditions necessary for the existence of space-time harmonics. This model is an idealization of a tube having two electron beams where the periodic variation of the dc parameters of the inner beam is provided by a bunched hollow outer beam. Since the periodic variation of the inner beam results from the moving electric field of the bunched beam rather than stationary electric or magnetic fields, the device illustrates an application of space-time harmonics rather than space harmonics and introduces a new method of providing the required periodic variations. A small signal analysis of the model leads to vanishingly small expressions for the amplitudes of the $n = 1, 2, \ldots$ space-time harmonics, and hence to the conclusion that for the model considered amplification over a wide band of frequencies is not practical.

ASD-TDR-63-527

TABLE OF CONTENTS

LIST OF ILLUSTRATIONS

I. INTRODUCTION

The presence of fast and slow space-charge waves on an electron beam as shown by Hahn[1] and Ramo[2] has led to the extensive investigation of their properties. Several authors[3-6] have predicted the existence of space-harmonics of the space-charge waves when an electron beam passes through a periodic field due to a stationary structure. Staprans and Mueller[7,8] have experimentally verified the existence of these space-harmonics and Mueller[9] has described their consequences in electron tubes.

Recently Mueller[10] has extended the analysis to space-time harmonics which occur when an electron beam is passed through a moving structure so that the beam sees a moving periodic field due to the moving structure.

The purpose of this report is two-fold: First, to illustrate an application of space-time harmonics in an electron beam tube and second, to derive expressions for the amplitudes of the space-time harmonics where the moving structure is itself an electron beam. An experimental tube was designed to amplify high-frequency signals (for the particular tube, 24 Gc.) over a fairly large bandwidth. A large class of tubes requires a slow-wave structure such as a helix so that the electromagnetic wave may have an axial phase velocity very nearly equal to the dc velocity of an axial electron beam. The dimensions of the slow-wave circuits become smaller as the frequency is increased, resulting in structures which are often difficult to fabricate. Unlike this class of tubes, in the experimental tube using space-time harmonics interaction occurs in a smooth cylindrical waveguide which for higher frequencies is simply made smaller in diameter, a feature making the experimental tube potentially practical for high-frequency operation. Some tubes have a narrow bandwidth, for example, the two-cavity klystron, while other tubes such as the TWT are capable of operating over a broad band of frequencies.

The experimental tube using space-time harmonics is of the latter type, that is, interaction between a harmonic on the beam and a mode in a waveguide may occur over a wide range of frequencies.

Unfortunately, the experimental tube failed to work, apparently due to the small amplitudes of the harmonics, as discussed in detail in Section IV. C.

The report is presented in three sections. First, a qualitative discussion of the operation of the tube is given and its behavior is compared to an ordinary TWT. The purpose of this section is to present a graphic picture of the operation of the tube and to introduce the space-time harmonics. Second, the properties of these harmonics are presented. Third, a quantitative discussion of the tube is given, in which the amplitudes of the harmonics are estimated and some of the experimental methods and results are presented. In addition to deriving an explicit formula relating the velocities of the two beams and the frequencies of the two electromagnetic waves special attention is given to the limiting perveance of the beams in the cylindrical waveguide.

Although the tube was designed to operate using the space-time harmonics of space-charge waves it may also operate in an entirely different manner, by considering one beam as a periodic structure through which the electromagnetic wave travels. To complete the discussion of the experimental tubes, this latter mode of operation is briefly considered in the Appendix.

II. QUALITATIVE DESCRIPTION OF THE EXPERIMENTAL TUBE

A. Physical Description of the Tube

Figure 1 shows the various elements within the tube and gives the dc potentials on the elements. A weak electromagnetic signal is fed in one end of the cylindrical waveguide, interacts with a harmonic as it travels down the guide, and leaves at the far end of the waveguide.

The second electron gun produces a hollow beam which passes successively through a helix and cylindrical waveguide to the collector as shown in Fig. 1. The hollow beam travels in synchronism with the circuit wave on the helix so that as it leaves the helix it has become bunched, i. e., the slow space-charge wave on the hollow beam is excited and amplified. The function of the helix is to bunch the hollow beam (not to amplify the electromagnetic wave on the circuit) so that when the hollow beam later passes through the waveguide it is bunched.

The first electron gun produces an inner beam which passes successively through the second gun, the helix, and the cylindrical waveguide to the collector. Unlike the hollow beam, the inner beam does not interact with the circuit wave on the helix because the inner beam is traveling much faster than the synchronous velocity, having been accelerated by the anode to cathode voltage of the first gun in addition to the anode to cathode voltage of the second gun.

Therefore, in the cylindrical waveguide a bunched hollow beam is moving rather slowly, an inner beam is moving much more rapidly, and an electromagnetic wave has an axial phase velocity greater than the speed of light. The electromagnetic wave is the signal to be amplified and it is a TM_{01} mode. One way of analyzing the interaction of the hollow beam, inner beam, and TM_{01} mode is to break the interaction into two steps: first, the bunched hollow beam interacts with the inner beam to satisfy the requirements for the existence of a set of harmonics on the inner beam; second, one of the harmonics is picked out, the -1 harmonic for example, and it is excited by and interacts with the electromagnetic wave. (The interaction between the electromagnetic wave traveling down the cylindrical waveguide and the -1 harmonic is very similar to the interaction of the circuit wave on a helix and the slow space-charge wave on an electron beam in the ordinary TWT.) To summarize, the bunched hollow beam interacts with the inner beam producing conditions for harmonics on the inner beam and one of the harmonics interacts with the TM_{01} mode resulting in gain (in a manner similar to a TWT).

first electron gun

second electron gun

collector

cylindrical waveguide

signal in

helix

amplified signal out

3 kv

5 kv

2.5 kv

200 volts

Electromagnetic wave (3 Gc, 1 watt)
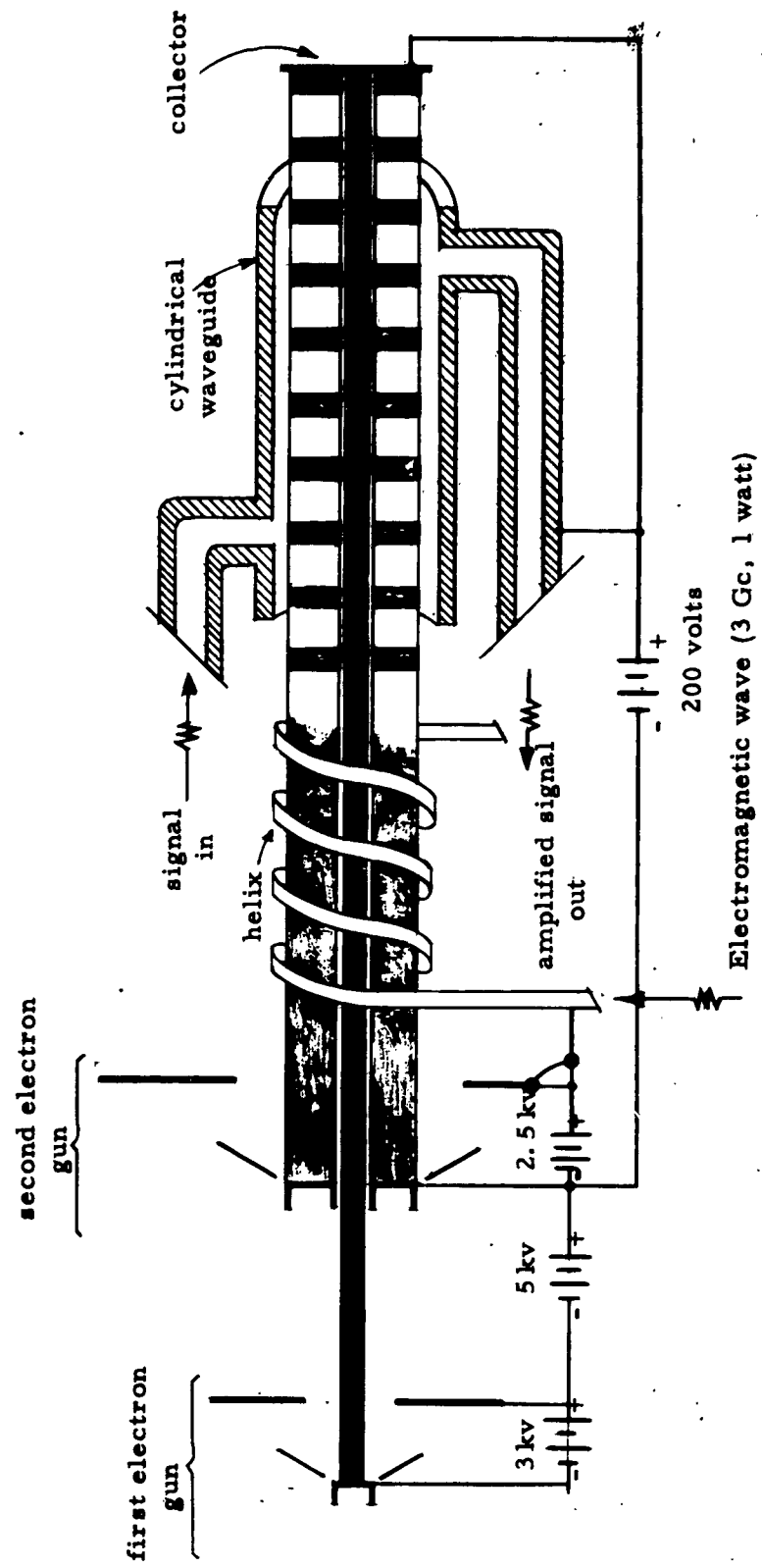
(Note: dc voltages for −1 harmonic interaction, see Fig. 3a)

Fig. 1 Cross-section of tube employing the space-time harmonics of the space-charge waves.

4

B. Representation of the Harmonics on ω-β Diagrams

This interaction between the two beams and the TM_{01} mode relies on some of the properties of the harmonics, or as they should be more completely called, the space-time harmonics of space-charge waves. The tube illustrates one means of setting up the conditions for their existence, namely, by using two beams, one passing through the second (a bunched beam) with a dc velocity different from that of the second beam. It also illustrates a method of exciting the harmonics, with a TM_{01} mode in a cylindrical waveguide. In a qualitative way ω-β diagrams show the properties of the harmonics which permit interaction of an electron beam with a wave traveling with an axial phase velocity greater than the speed of light. Figure 2 compares the harmonics with the slow and fast space-charge waves. In Fig. 2a is shown the ordinary slow space-charge wave (the dashed line indicates it has negative kinetic energy[7]) and the fast space-charge wave (the solid line indicates it has positive kinetic energy). Figure 2b shows a set of harmonics which are seen to occur in pairs, each pair consisting of a negative kinetic energy wave and a positive kinetic energy wave, and each pair identified by an integer n. The two waves corresponding to the n= 0 harmonics appear similar to the ordinary space-charge waves of Fig. 2a, as indeed they are, but they are different in that the amplitudes of the harmonics are different from the amplitudes of the slow and fast space-charge waves, information not shown by an ω-β diagram. The ω-β diagrams show the dependence of β on ω graphically, a relation derived later analytically as Eq. (2. 26).

In Figs. 3a and 3b the ω-β diagram for a set of harmonics and the TM_{01} mode in a cylindrical waveguide are superimposed. In Fig. 3a the dc velocity is such that the -1 harmonic interacts with the TM_{01} mode while in Fig. 3b the dc velocity of the beam is decreased and the -2 harmonic interacts with the TM_{01} mode
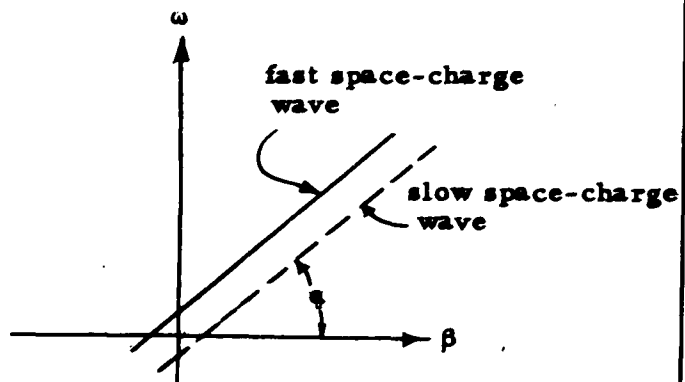
Fig. 2a   Space-charge waves

Fig. 2b   Space-time harmonics of space-
charge waves

Fig. 3a Interaction between TM$_{01}$ mode and -1 harmonic

Fig. 3b Interaction between TM$_{01}$ mode and -2 harmonic
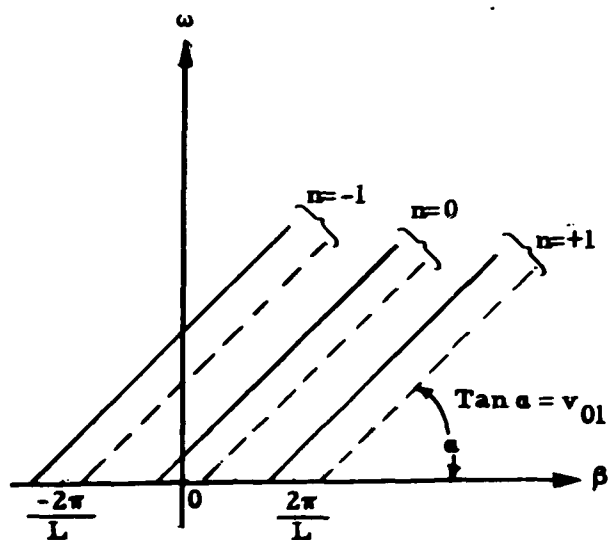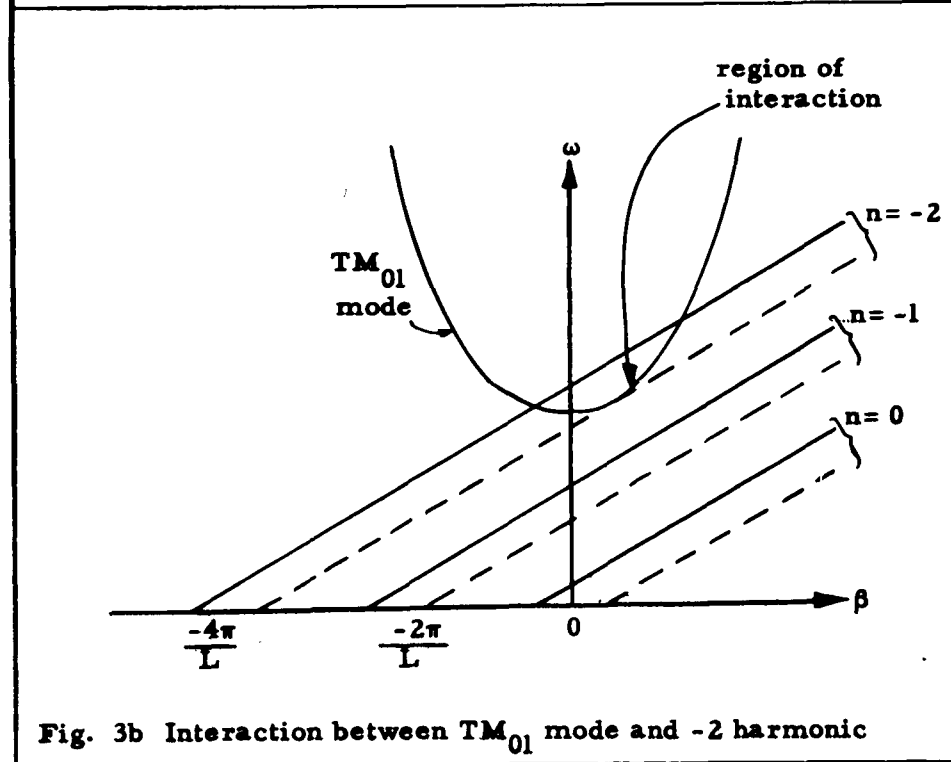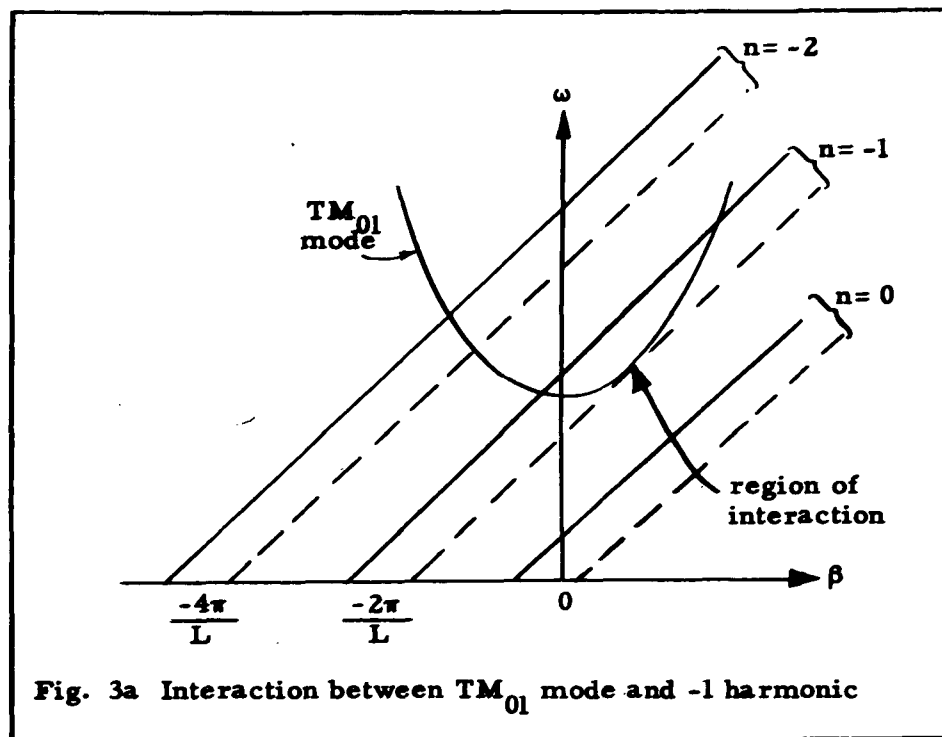
at the same signal frequency. These diagrams illustrate graph-
ically the interaction between the inner beam and the hollow outer
bunched beam by the set of parallel lines representing the space-
time harmonics. The region of interaction of the TM_{01} mode and
a harmonic on the inner beam is also shown on the $\omega-\beta$ diagram.

C. Relative Amplitudes of the Harmonics

One feature of importance the $\omega-\beta$ diagrams do not show
is the relative amplitudes of the harmonics; the reason the ex-
perimental tube failed to work was that the amplitudes were not
large enough. To clarify what is meant by the amplitudes of the
harmonics, the experimental tube can be compared with the or-
dinary TWT. For small signals the total charge density of the
electron beam of the TWT is usually divided into an ac term ρ and
a large dc term ρ_0 so that the total charge density is given by

$$\rho_T = \rho_0 + \rho \tag{2.1}$$

The velocity and current of the beam may in a similar manner be
divided into dc and ac terms. For a TWT where only the slow
space-charge wave is excited the total charge density has the form

$$\rho_T = \rho_0 + |\rho| e^{-j(\beta z - \omega t)} \tag{2.2}$$

In a beam which is split up into harmonics the correspond-
ing equation for the charge density has the form

$$\rho_T = \rho_0 + \sum_{n=-\infty}^{\infty} |\rho| J_n \left(\frac{L\Delta\beta}{2\pi} \right) e^{-j(\beta_n z - \omega t)} \tag{2.3}$$

where in each pair of waves corresponding to an integer n only
the wave of negative kinetic energy is excited and the wave of
positive kinetic energy is not excited and hence omitted. Com-
paring Eqs. (2.2) and (2.3) one notes that the amplitude of the
ac charge density of a harmonic is proportional to a Bessel func-
tion of order n with argument $(L\Delta\beta)/(2\pi)$, while the amplitude

- 8 -

of the traveling-wave tube's ac charge density does not depend on any Bessel function. In the experimental tube the value of the Bessel function for $n = 1$ was approximately 10^{-4} so that the amplitude of the harmonic was vanishingly small, a value determined after the tube was built (see Sec. IV. C).

III. THE SPACE-TIME HARMONICS OF SPACE-CHARGE WAVES[10]

A. Frames of Reference

The experimental tube described in the previous section is an example of a specific application of the space-time har-. . monics. The harmonics will be approached from a more general point of view to explain not only the operation of the experimental tube but to provide a basis for possible modifications of the tube.

In this section equations are developed for transforming quantities such as ω and β from one frame of reference to another and a particular frame of reference is chosen which simplifies the calculations. In later sections restrictions are applied which lead to equations for space-time harmonics and the properties of these harmonics are then considered with special attention to their applications to electron devices. It is shown that the nth harmonic will consist of a pair of waves which has many of the characteristics of the fast and slow space-charge waves.

Two frames of reference shall be used: A stationary system denoted by X and a system X' moving at a velocity v_w with respect to X. The position (x, y, z) and time t in system X can be related to the position (x', y', z') and time t' in system X' by the Lorentz transformations[11] as follows

$$z = k(z' + v_w t')$$

$$t = k(t' + \frac{v_w}{c^2} z')$$

$$k = \frac{1}{\sqrt{1 - (v_w/c)^2}} \qquad (3.1)$$

From Eq. (3.1) the velocity v in X can be determined when the velocity v' in X' is given as follows

$$v = \frac{dz}{dt} = \frac{k(dz' + v_w dt')}{k(dt' + \frac{v_w}{c^2} dz')} \qquad v = \frac{v' + v_w}{1 + \frac{v_w v'}{c^2}} \qquad (3.2)$$

By rearranging Eq. (3.2) the velocity v' in X' in terms of v in X is given as

$$v' = \frac{v - v_w}{1 - \frac{v_w v}{c^2}} \qquad (3.3)$$

The amplitude and phase of a wave are invariant under transformation so that

$$A e^{j(\omega t - \beta z)} = A' e^{j(\omega' t' - \beta' z')} \qquad (3.4)$$

$$A = A' \qquad (\omega t - \beta z) = (\omega' t' - \beta' z')$$

From the above equations the frequency ω in X in terms of quantities X' is

$$\omega = k\omega' (1 + \frac{v_w}{v'}) \qquad (3.5)$$

These equations transform a wave from one frame of reference to another. Of particular interest is the transformation of the harmonics of space-charge waves. Therefore the additional relation

$$\omega'_\rho = \omega_\rho (\frac{1}{\sqrt{1 - (v'_e / c)^2}}) \qquad (3.6)$$

is useful. The plasma frequency is $\omega_\rho = \sqrt{\eta \rho / \epsilon_0}$, and v'_e is the velocity of the beam as seen by an observer in X'. For relativistic velocities ρ is the charge density in a system traveling with the electrons.

The frames of reference are introduced to simplify the discussion of the class of tubes which have a beam moving along

the z-axis with a dc velocity $\bar{v}_e$ with respect to the laboratory and also have a structure moving at velocity v_w in the z direction. The laboratory is chosen as system X. The system X' is chosen so that the structure appears stationary to an observer in X', i. e., X' is moving with the structure at a velocity v_w with respect to the laboratory. At this point it is not necessary to specify just what the structure is, and to achieve generality the discussion is not limited to just one structure. (One possible structure is the hollow bunched beam of the experimental tube.)

As yet no restriction has been placed on v_w. If v_w is positive the structure moves toward the collector and if v_w is negative the structure moves towards the cathode. In the special case where v_w is zero, the structure is stationary with respect to the laboratory and systems X and X' are identical. To an observer in X' the beam will have an apparent velocity

$$\bar{v}'_e = \frac{\bar{v}_e - v_w}{1 - \frac{\bar{v}_e v_w}{c^2}} \tag{3.7}$$

which follows directly from Eq. (3. 3).

To summarize, in this section formulae have been developed for transformation of waves from one system to another, where system X is the laboratory frame of reference and system X' is moving with the structure.

B. Restrictions on the Structure

Provided three restrictions on a structure are satisfied, a beam may have space-time harmonics as it passes through the structure.

First, the structure must move at a velocity v_w which is not equal to the velocity of the beam v_e. This condition states that

$$\text{in system X: } \bar{v}_e \neq v_w$$

$$\text{or in system X': } \bar{v}'_e \neq 0 \tag{3.8}$$

One special case of interest is for v_w to equal zero, i.e., for the structure to be stationary.

Second, an observer in X' (moving with the structure) should see a periodic variation in the voltage along the axis of the tube due to the fields on the structure. Let L' be the period of the spatial periodicity and $\Delta \hat{V}_0$ be the voltage due to the structure so that in X'

$$\Delta \hat{V}'_0(z') = \Delta \hat{V}'_0(z' + L') \tag{3.9}$$

Since this voltage is periodic it may be represented by a Fourier series, so the special case of a sinusoidal variation is of interest:

$$\Delta \hat{V}'_0(z') = \Delta \hat{V}'_0 \sin\frac{2\pi z'}{L'} \tag{3.10}$$

Third, the magnitude of $\Delta \hat{V}'_0$ should be less than $\bar{V}'_0$ where $\bar{V}'_0$ is the voltage through which the beam is accelerated by the electron gun ($v_e = \sqrt{2\eta \bar{V}'_0}$). That is

$$\Delta \hat{V}'_0 < V'_0 \tag{3.11}$$

Example 1.
_____

In Fig. 4 is shown a structure which satisfies these three conditions. A stationary set of apertured disks is arranged so that the beam may pass through the center of the disks. Voltages on the disks are adjusted so that on the axis of the tube there is essentially a sinusoidal voltage variation due to the disks. Figure 4 illustrates one method of meeting the requirements necessary for the existence of the harmonics but it does not show a complete tube as no method of exciting the space harmonics or of amplifying them is shown. (Analogously an ordinary beam in a drift tube does not necessarily have a slow space-charge wave on it. It is necessary to pass the beam through a modulating circuit

- 12 -
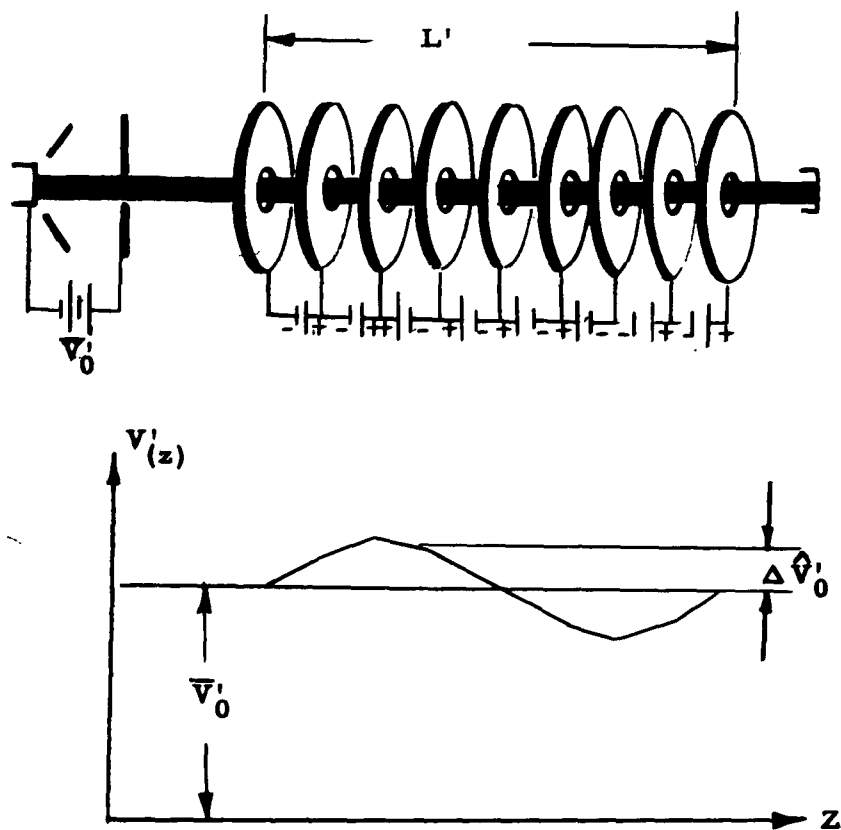
Restrictions

(1) $v_w \neq v_e$ (for stationary structure $v_w = 0$)

(2) $\Delta \hat{V}_0(z') = \Delta \hat{V}_0' \sin \dfrac{2\pi z'}{L'}$

(3) $\Delta \hat{V}_0' < \overline{V}_0'$

Fig. 4   Electron beam through a series of apertured disks

such as a helix or across a gap of a cavity to actually excite the waves.) If the set of apertured disks are stationary then v_w is zero. This special case is distinguished from the more general case where v_w is not necessarily zero by calling the harmonics space harmonics. (Space harmonics are a special case of the more general space-time harmonics.)

Example 2.

Figure 5. shows another structure which satisfies the three conditions. An outer hollow beam has been bunched and surrounds an inner beam. In this case the outer beam can move with a velocity faster or slower than the inner beam but by the first restriction it cannot move with exactly the same velocity as the inner beam. (In the experimental tube considered in Sec. I the outer hollow beam moved slower than the inner beam due to the arrangement of the electron guns (see Fig. 1). The experimental tube is a special case of the example considered here.) The field due to the bunched hollow beam results in a periodic variation in the field along the z-axis and hence V_0' along the z-axis. As seen by an observer in X' (moving with the bunched beam) the variation is stationary and does not change with time, while to an observer in X (the laboratory system) the pattern appears to be moving slightly slower than the dc velocity of the hollow beam. Figure 5 illustrates a method of meeting the requirements for the existence of space-time harmonics but it does not show a complete tube as no method of exciting the space harmonics has been indicated. (One method to excite the harmonics is with a TM_{01} mode as in the experimental tube.)

The above examples have been given to illustrate the three necessary conditions for the existence of space-time harmonics.
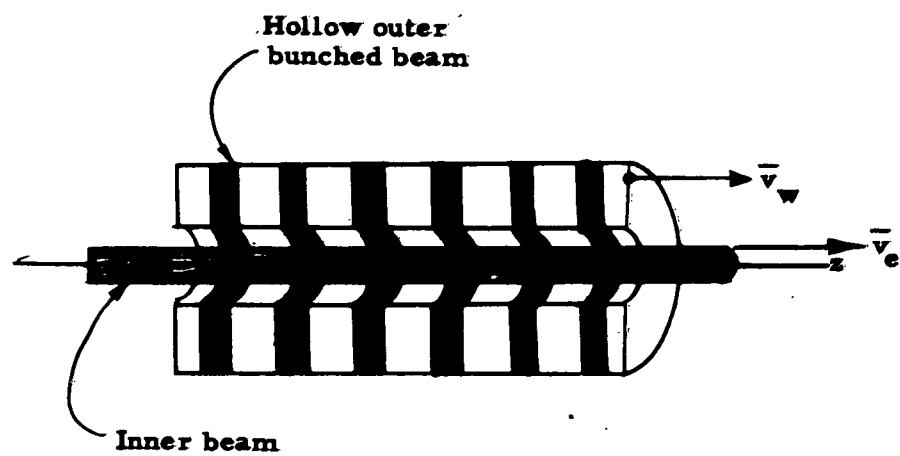
- 14 -

Fig. 5 Half section of outer beam surrounding an inner beam

C. Space Harmonics of Apertured Disks

The phase constants of the space-charge waves are given by

$$\beta = \frac{\omega \pm \omega_p}{\bar{v}_e} \qquad (3.12)$$

where $\bar{v}_e = \sqrt{2\eta \bar{V}_0}$ is the dc velocity of the beam.

But if the beam is passing through a structure which has a periodic voltage along the axis as given by Eq. (3.9) then the above equation must be modified. For the special case where the periodic voltage is sinusoidal then

$$\beta(z) = \frac{\omega \pm \omega_p}{v_e(z)} \qquad (3.13)$$

where

$$v_e(z) = \sqrt{2\eta(\bar{V}_0 - \Delta\hat{V}_0 \sin\frac{2\pi z}{L})} = \bar{v}_e(1 - \frac{\Delta\hat{V}_0}{\bar{V}_0}\sin\frac{2\pi z}{L})^{\frac{1}{2}}$$

There is an additional term in the above equation due to the periodic voltage on the axis. If $\Delta\hat{V}_0 < \bar{V}_0$ then by discarding higher powers of $\Delta\hat{V}_0/\bar{V}_0$ one gets

$$\beta = \frac{\omega \pm \omega_p}{\bar{v}_e}(1 + \frac{1}{2}\frac{\Delta\hat{V}_0}{\bar{V}_0}\sin\frac{2\pi z}{L}) \qquad (3.14)$$

or

$$\beta = \beta_0 + \Delta\beta \sin\frac{2\pi z}{L}$$

where

$$\beta_0 = \frac{\omega \pm \omega_p}{\bar{v}_e} \qquad\qquad \Delta\beta = \beta_0\frac{\Delta\hat{V}_0}{2\bar{V}_0}$$

For Eq. (3.14) to be finite it is necessary that $\bar{v}_e \neq 0$. This is the first restriction on the structure considered in Sec. B. It implies that $\bar{v}_w \neq \bar{v}_e$, that the beam moves at a different velocity than the structure.

For small-signal analysis the charge density, velocity, and current of the beam may be divided into dc and ac terms. Therefore,

$$i_T = i_0 + i = i_0 + |i| \ e^{j[\omega t - \int_0^z \beta(z) \, dz]} \tag{3.15}$$

Hereafter the dc term will be neglected, a procedure which is justified for small signals. (Note that if $\Delta \hat{V}_0 \approx \bar{V}_0$ then the problem would be outside the range of small-signal analysis. This is the reason for the third restriction on the structure. Also if $\Delta \hat{V}_0 \approx \bar{V}_0$ it would not be possible to discard higher order powers of $\Delta \hat{V}_0 / \bar{V}_0$ as was done in Eq. (3.14).) The ac portion of Eq. (3.15) is

$$i = |i| \ e^{j[\omega t - \int_0^z (\beta_0 + \Delta\beta \ \sin \frac{2\pi z}{L}) \, dz]} \tag{3.16}$$

In the above equation note that an integral is necessary since $\beta(z)$ is a function of z. [12] This is similar to replacing ωt by $\int_0^t \omega(t) \, dt$ in frequency modulation.

A mathematical identity states that

$$e^{-j[\beta_0 z - \frac{L\Delta\beta}{2\pi} \cos \frac{2\pi z}{L}]} = \sum_{n=-\infty}^{+\infty} J_n(\frac{L\Delta\beta}{2\pi}) \ e^{-j(\beta_0 + \frac{2\pi n}{L})z} \tag{3.17}$$

Using this identity the ac current may be written as a series of terms:

$$i = |i| \sum_{n=-\infty}^{\infty} J_n(\frac{L\Delta\beta}{2\pi}) \ e^{j(\omega t - \beta_0 z - \frac{2\pi n z}{L})} \tag{3.18}$$

This is the fundamental equation for the space-time harmonic current. Each term in the series is a harmonic. For example, an equation which completely describes the ac current density of the -1 harmonic is

$$i_{-1} = |i| \ J_1(\frac{L\Delta\beta}{2\pi}) \ e^{j(\omega t - \beta_0 z + \frac{2\pi z}{L})} \tag{3.19}$$

The derivation of the harmonics proceeded directly from Eq. (3.12) rather than starting from Maxwell's equations. In the

derivation the three restrictions in the mathematics correspond to the three restrictions that were placed on the structure. In Sec. B these three restrictions are stated without being justified, but in this section it becomes clear that they are necessary if one is to have harmonics. Thus these restrictions provide a useful criteria for evaluating structures proposed for space-time harmonic amplification.

The current variation consists of an infinite number of space harmonics whose amplitudes are given by various order Bessel functions. Note that the complete sum of all the space harmonics together make up the current variation. Hence these space harmonics are sometimes called "partial" waves. For brevity two equations have been written as one. That is, $\beta_0 = (\omega \pm \omega_p)/\bar{v}_e$ means $\beta_0 = (\omega + \omega_p)/\bar{v}_e$ and $\beta_0 = (\omega - \omega_p)/\bar{v}_e$. Equation (3.18) written out as two equations would be

$$i_n = |i| \sum_{n=-\infty}^{\infty} J_n \left(\frac{L\Delta\hat{V}_0}{4\pi\bar{V}_0} \frac{\omega+\omega_p}{\bar{v}_e} \right) e^{j(\omega t - \beta_{nn} z)} \qquad (3.20)$$

where

$$\beta_{nn} = \frac{\omega+\omega_p}{\bar{v}_e} + \frac{2\pi n}{L}$$

and

$$i_p = |i| \sum_{n=-\infty}^{\infty} J_n \left(\frac{L\Delta\hat{V}_0}{4\pi\bar{V}_0} \frac{\omega-\omega_p}{\bar{v}_e} \right) e^{j(\omega t - \beta_{np} z)} \qquad (3.21)$$

where

$$\beta_{np} = \frac{\omega-\omega_p}{\bar{v}_e} + \frac{2\pi n}{L}$$

Equation (3.21) corresponds to all harmonics which have positive kinetic energy and Eq. (3.20) to all those that have negative kinetic energy.[13] The practical result is that it is possible to excite only the positive or the negative set (just as it is possible to excite only the fast or the slow space-charge wave). However, the above equations show that the waves of each set are related. That is, suppose that J_{-1n} is replaced by $2J_{-1n}$ but that β remains

unchanged. Physically this means that we amplify the -1 space
harmonic which has negative kinetic energy -- which is the case
in the experimental tube. Then the mathematical identity (Eq.
3. 21) requires that all the other negative-kinetic-energy space
harmonics and the left-hand side of the equation be doubled. That
is, the amplitude of one harmonic will not change unless the am-
plitudes of all harmonics with the same kinetic energy change in
the same ratio, provided β remains unchanged.

The amplitudes of these space harmonics can be com-
pared with the sidebands of frequency modulation. By a proper
choice of the argument one can make the amplitude of any har-
monic go to zero. Actually this happens at the zeros of the Bes-
sel functions, i. e., the first harmonic goes to zero when
$(L\Delta\beta/2\pi)$ has a value that makes $J_1(L\Delta\beta/2\pi)$ zero. Clearly, if
one is interested in amplifying a specific harmonic, low values
of its amplitude are avoided. (The best argument to choose to
amplify a harmonic is found by differentiating the corresponding
Bessel function and setting the derivative equal to zero.)

There is another useful feature which can be drawn from
frequency modulation to understand the nature of space harmonics.
In FM one convenient way to represent the sidebands is by a
frequency spectrum of the wave. In a similar manner one can
represent the space harmonics by a "β spectrum". The analogy
between space harmonics and sidebands is shown in Fig. 6.

In the experimental tube the argument $(L\Delta\beta/2\pi)$ was far
from the optimum value described above. Other factors in the
tube, primarily the low plasma frequency of the hollow beam,
resulted in a very low value of the argument.

A relation between β and ω is also given by Eqs. (3. 20)
and (3. 21). Noting that $\omega_n = \overline{v}_e \beta_n$ one has

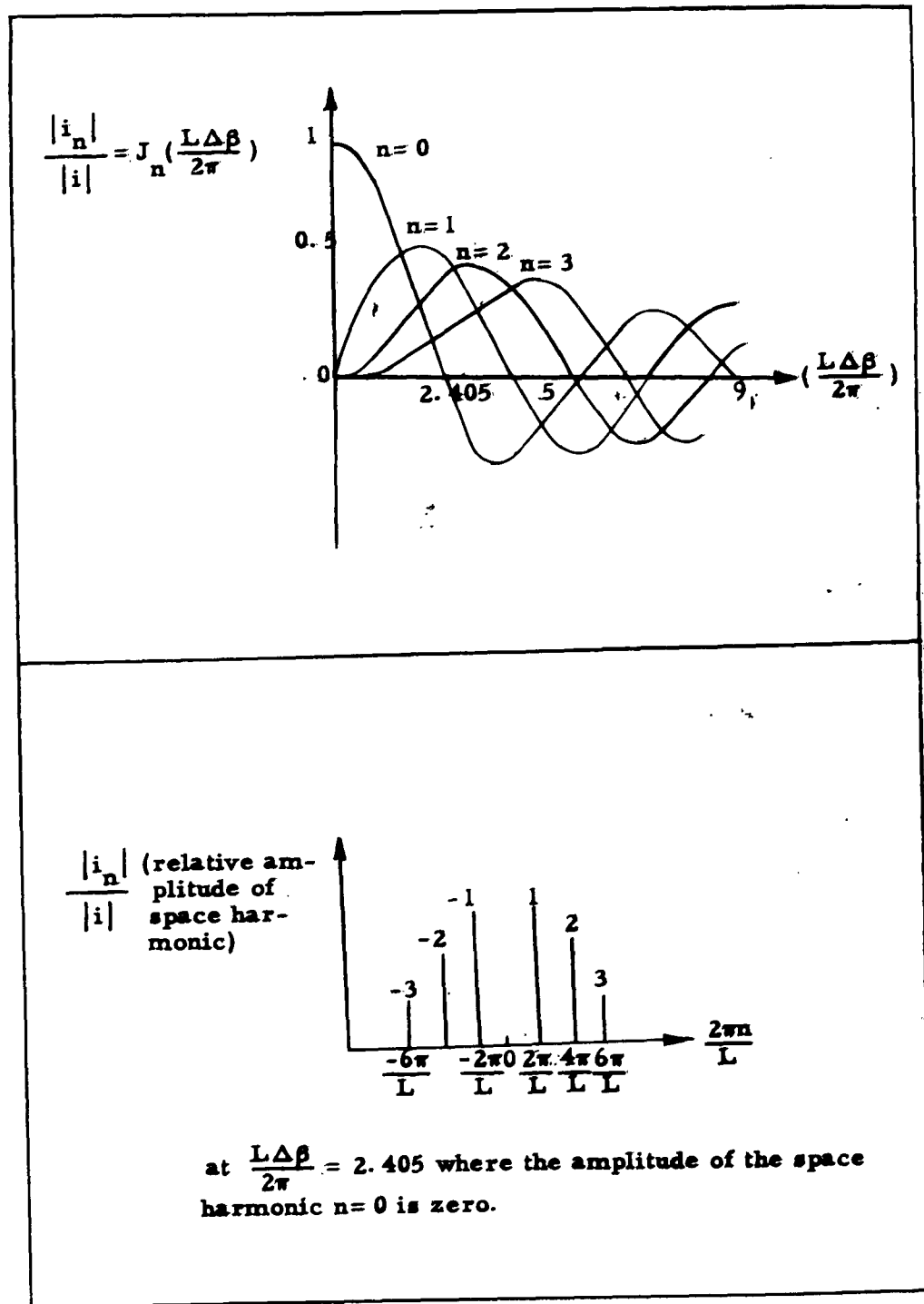$$\omega_n = \overline{v}_e \left(\frac{\omega + \omega_p}{\overline{v}_e} + \frac{2\pi n}{L} \right) \tag{3. 22}$$

$$\frac{\left|i_n\right|}{\left|i\right|} = J_n\left(\frac{L\Delta\beta}{2\pi}\right)$$

n= 0

0.5

n= 1

n= 2 n= 3

0

2.405   5   9 $\left(\frac{L\Delta\beta}{2\pi}\right)$

1

$\frac{\left|i_n\right|}{\left|i\right|}$ (relative amplitude of space harmonic)

-1

-2

1

2

-3

3

$\frac{2\pi n}{L}$

$\frac{-6\pi}{L}$ $\frac{-2\pi}{L}$ 0 $\frac{2\pi}{L}$ $\frac{4\pi}{L}$ $\frac{6\pi}{L}$

at $\frac{L\Delta\beta}{2\pi} = 2.405$ where the amplitude of the space harmonic n= 0 is zero.

Fig. 6 Amplitudes of space harmonics

This relation can be represented graphically by an ω-β diagram as shown in Fig. 2b.

In conclusion, three important properties of the harmonics are:

First, if $\beta(z)$ remains unchanged, the amplitude of one harmonic with negative kinetic energy will not change unless the amplitudes of all the harmonics with negative kinetic energy change in the same ratio. A similar statement is true for positive kinetic energy waves.

Second, the magnitude of the nth harmonic is given by a Bessel function of order n with argument $(L\Delta\beta/2\pi)$. One graphic representation of the amplitudes is provided by a β spectrum as in Fig. 6.

Third, a relation between ω and β can be graphically expressed by an ω-β diagram or can be found from Eq. (3. 22).

D. Transformation of Space-Time Harmonics

For the special case $v_w = 0$, i. e., the structure is stationary with respect to the laboratory, an example of which was the set of apertured disks discussed in Secs. B and C, the transformation from system X to X' merely consists of adding primes on all the quantities v, ω, β, β_0, z and L which appear in the equations of Sec. C. For $v_w = 0$ it makes little difference whether one derives the equations for the harmonics in system X or X'.

But if $v_w \neq 0$ then it is much easier to derive the equations for the space-time harmonics in system X' and then transform them by the equations of Sec. II. B into system X rather than attempting to derive the space-time harmonics directly in system X. The material on space harmonics in Sec. III. C has been considered for the special case $v_w = 0$, whereas space-time harmonics arise for any value of v_w.

$v_w \neq 0$ implies a moving structure and X' is the one frame of reference which moves with the structure. In system X', $\Delta\hat{V}_0$

is a function of z only and not of t, that is, the periodic voltage appears stationary in space. For example, an observer moving with nearly the dc velocity of the bunched hollow beam in the experimental tube sees a stationary periodic space distribution of bunched electrons. To be concise, replace all quantities in Sec. C by their primes, e. g., Eq. (3.18) becomes

$$i' = \sum_{n=-\infty}^{\infty} |i'| \; J_n(\frac{L'\Delta\beta'}{2\pi}) \, e^{j(\omega_n' t' - \beta_n' z')}$$

(3.23)

where

$$\omega_n' = \omega, \quad \beta_n' = \beta_0 + \frac{2\pi n}{L}$$

and the rewritten equations will give the space-time harmonics in system X'.

As all measurements are made in the laboratory frame of reference X, it is desirable to transform the equations from the moving system X' to system X. This is accomplished by using the Lorentz transformations in Sec. A to get, for instance,

$$\omega_n = \omega_0 + n\omega_w = \beta_n \overline{v}_e \pm \frac{\omega_p}{k_e} + (1 - \frac{\overline{v}_e}{v_w}) \, n\omega_w$$

(3.24)

Figures 7a and 7b show a graphic representation of these relations between ω and β by an ω-β diagram. In Fig. 7a is shown the system X' moving at velocity v_w. The signal is excited on one harmonic at point A. In Fig. 7b the same spectrum has been transformed by Eq. (2.26) to the laboratory frame of reference, system X. Since the waves of like kinetic energy are all related, if one is excited so are all the others. But note that the signal appears at a different frequency on the different harmonics as seen from the laboratory frame of reference. This leads to the possibility of frequency conversion, by placing the signal on one harmonic at the frequency ω_1, and removing it from another harmonic at frequency ω_2.
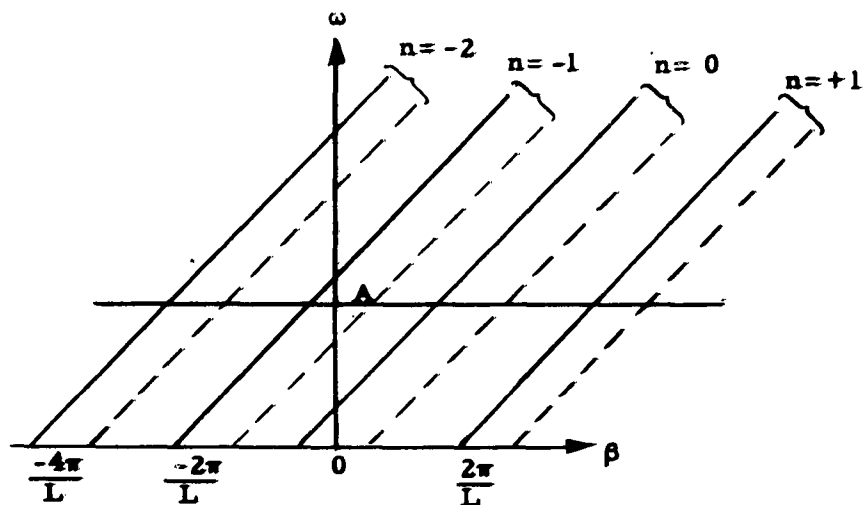
ω-β diagram as seen by an observer moving with the system X'. (Note that in each pair of harmonics only one wave is excited. This corresponds to the special case of the experimental tube.)

Fig. 7a System X' moving at velocity v_w.
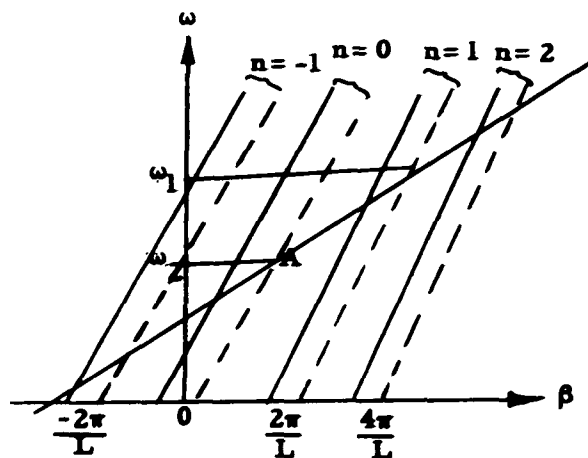
ω-β diagram for the same set of harmonics as in Fig. 7a but now seen by an observer in the laboratory frame of reference.

Fig. 7b System X Nonmoving

Another application of space-time harmonics would be to excite a harmonic at frequency ω_1 and then amplify at a lower frequency ω_2 of another harmonic, since the signal will also appear on this harmonic, and finally, since all the harmonics have been amplified, to remove the now amplified signal at frequency ω_1. That is, a high-frequency signal is amplified by a low-frequency source.

Therefore, one additional property that space-time harmonics have when $v_w \neq 0$ is that the set of harmonics which are excited as a group will have signals at different frequencies as given explicitly by Eq. (3.24). However, in the experimental tube use was not made of this particular property.

In the experimental tube, $v_w \neq 0$ as the dc velocity of the hollow beam corresponds to v_w, i.e., system X' moves with the hollow beam. Therefore, a rigorous analysis would require the use of space-time harmonics rather than the simpler space harmonics. However, in the experimental tube no use is made of properties of space-time harmonics which are not also properties of space harmonics, since if v_w is small compared with the velocity of the electron beam passing through the structure, v_e, $v_w \ll v_e$, then to a first approximation the harmonics may be considered to be space harmonics.

IV. QUANTITATIVE DESCRIPTION OF THE EXPERIMENTAL TUBE

A. RF Transmission.

Figure 8 shows the RF circuit for the signal. The purpose of this experiment was to determine if a signal could be coupled from a TE_{10} mode in a rectangular guide to a TM_{01} mode in a cylindrical guide and then in turn to a TE_{10} mode in a rectangular guide without excessive loss. Since the measurements were made before the waveguide was placed within the glass envelope, the opening between the rectangular and cylindrical waveguide could be blocked and then unblocked to determine the

signal in

glass

TE_{10} mode

TM_{01} mode in cylindrical waveguide

TE_{10} mode in rectangular waveguide

signal out
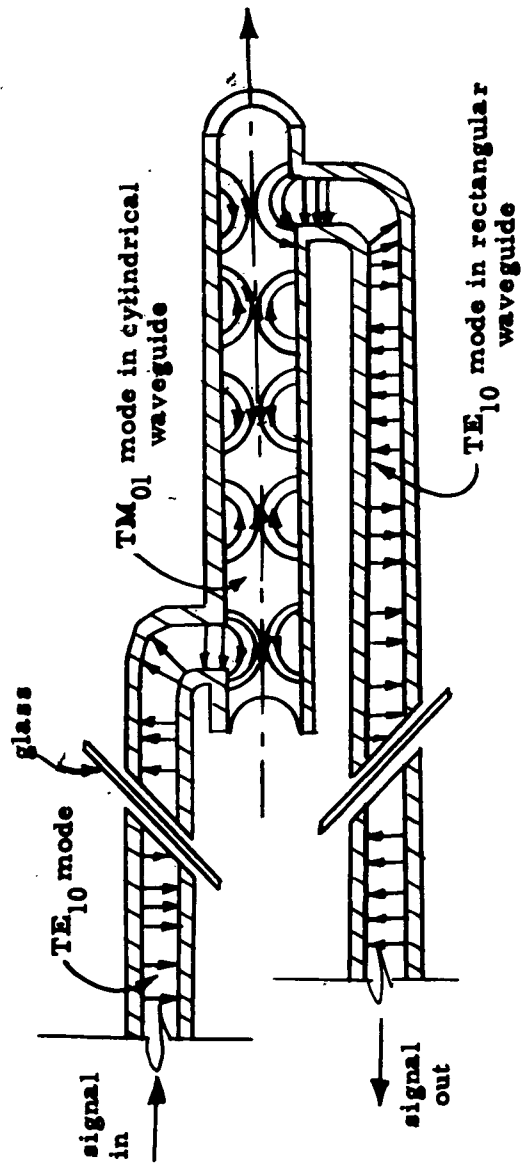
Fig. 8 RF circuit for signal

portion of the signal traveling through the tube. Transmission was adequate so that the coupling from the rectangular guide to the cylindrical guide did not have to be modified. The insertion loss was 20 db.

A TM_{01} mode of 24-Gc is 1.3 times the cutoff frequency of the waveguide and the coupling of the fields from the rectangular guide to the cylindrical guide is shown in Fig. 8, resulting in excitation of the TM_{01} mode within the guide. Higher-order modes are below cutoff and thus do not propagate.

B. Bunching of the Outer Beam

The purpose of the helix is to bunch the outer hollow beam. A helix of any convenient pitch may be chosen. The hollow beam, having a dc velocity slightly slower than the axial phase velocity of the 2.4-Gc signal on the helix, is bunched as it passes through the helix. Due to a difference of potential between the end of the helix and the cylindrical waveguide, the bunched beam is slowed down and more tightly bunched as it enters the waveguide. Choosing a rather coarse helix results in a large range of possible values for the dc velocity of the beam as it passes through the helix, but the dc velocity of the hollow beam as it enters the cylindrical waveguide (a velocity made as small as possible) is simply controlled by adjusting the potential between the helix and waveguide. Thus the dc velocity of the hollow beam within the helix is determined by the pitch of the particular helix but the pitch may be any convenient value.

1. Velocity jump between helix and waveguide

There exists a velocity jump between the end of the helix and the beginning of the cylindrical waveguide which slows down both the bunched hollow beam and the inner beam. The velocity jump serves the twofold purpose of decreasing the dc velocity of the hollow beam and decreasing the distance between space-charge bunches of the hollow beam. After passing through

the helix and velocity jump the hollow outer beam is _tightly bunched, and the period L is small._ Inside the cylindrical waveguide the inner solid beam moves rapidly through the tightly bunched outer beam.

2. Hollow beam in velocity-jump region

Figure 9 shows an idealized hollow beam as it travels through the helix, velocity-jump region, and cylindrical waveguide. A string of charge bunches moving with velocity $\bar{v}_{OH}$ and with period L_H leaves the right end of the helix, is slowed down by the electric field between the helix and waveguide, and proceeds with a decreased velocity $\bar{v}_{02}$ and a smaller period L. The time between the arrival at the waveguide of the successive spike bunches is $t = L/\bar{v}_{02}$, and the time between the departure at the helix of two successive bunches is given by $t_H = L_H/\bar{v}_{OH}$. The same number of bunches must arrive at the waveguide as leave the helix; therefore, the two times t and t_H must be equal, so that

$$L = \frac{\bar{v}_{02}}{\bar{v}_{OH}} L_H \qquad (4.1)$$

This same equation holds for the actual hollow beam as well as the idealized beam to a first approximation (i. e., lens effects are neglected) provided the dc velocity of the beam as it arrives at the waveguide is large enough so that the perveance is less than the limiting perveance. The period L_H is given by

$$L_H = \lambda_p = \frac{\bar{v}_{OH}}{f_H} \qquad (4.2)$$

where λ_p is the plasma wavelength of the hollow beam and f_H is the frequency of the electromagnetic wave on the helix (2.4 Gc). By combining Eqs. (4.1) and (4.2) the periodicity for the bunched beam within the cylindrical waveguide is

$$L = \frac{\bar{v}_{02}}{f_H} \qquad (4.3)$$

helix
hollow beam
bunched

velocity
jump
region

waveguide

ρ_m

L_H

1
2
3
4
5
6

A
B

$\rightarrow ||\leftarrow \phi$ (t = t_0)

dc component of beam not shown

ρ_m

spike beam

1
2
3
4
5
6

A
B

(t = t_0 + Δt)

ρ_m

1
2
3
4
5
6

A
B

(t = t_0 + 2Δt)
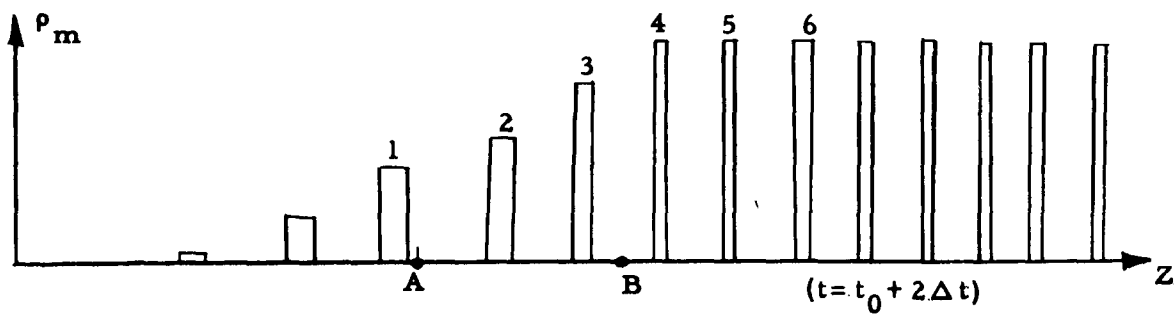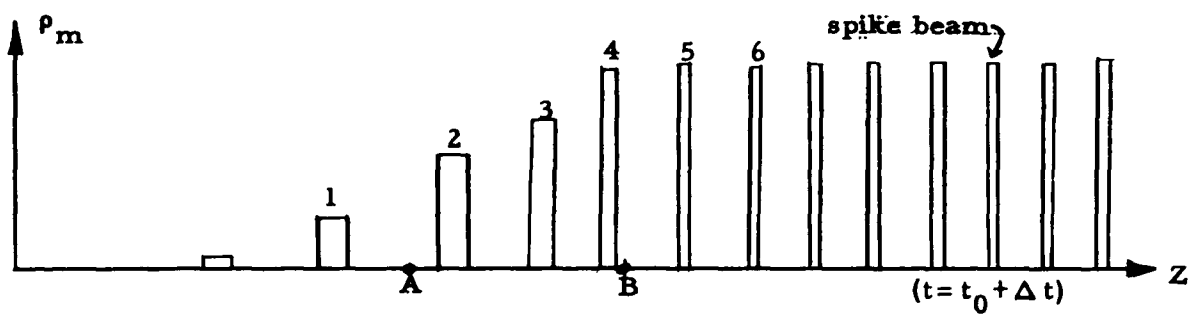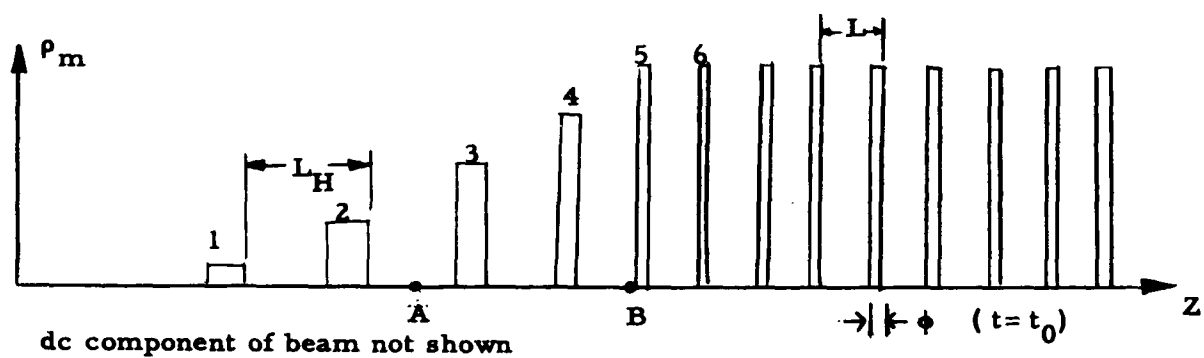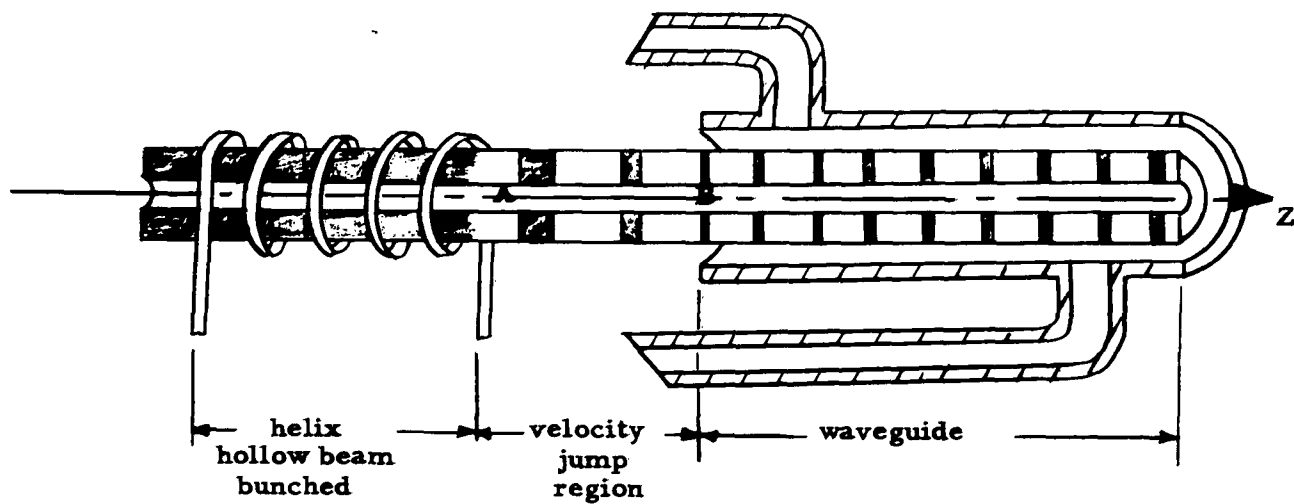
Fig. 9   Idealized Hollow Beam

- 28 -

This equation shows that the period L may be made small by slowing down the outer beam so that it has a small velocity $\bar{v}_{02}$ within the waveguide. The tightly bunched hollow beam sets up a periodic voltage on the axis, and the first component of the Fourier representation of the periodic field is the term $\Delta \hat{V}_0 \sin \frac{2\pi z}{L}$. That is, the hollow beam is the structure which sets up a periodic voltage on the axis. There are assumed to be no harmonics on the hollow beam.

3. Inner beam in velocity-jump region

There are harmonics on the inner beam at the right end of the helix, in the velocity-jump region, and within the cylindrical waveguide, since the inner beam is passing through a bunched outer beam, and the three restrictions on the structure discussed in Sec. III.B are satisfied. At the left end of the helix there are no harmonics as the inner beam passes through an unbunched outer beam. The magnitude of $\Delta \hat{V}_0$ increases from zero to a maximum value as the hollow beam becomes bunched. By the time the inner beam reaches the right end of the helix, the inner beam is passing through a bunched beam and has harmonics. Figure 10 shows the space-time harmonics on the inner beam at the right end of the helix and at the entrance to the cylindrical waveguide. Note that the slope of the harmonics is decreased owing to the decrease in the dc velocity of the inner beam but that the most important change is due to the decrease in the periodicity from L_H to L. This radical change in the periodicity is the reason for introducing the velocity-jump region.

As seen from the ω-β diagram in Fig. 10, the region of interaction between the -n harmonic and the TM_{01} mode is near the ω axis, so that to a first approximation β_n may be set equal to zero:

$$\beta_n = \beta_0 + \frac{2\pi n}{L} \approx 0 \qquad (\beta_0 = \frac{\omega + \omega_p}{\bar{v}_e} \approx \frac{\omega}{\bar{v}_e}) \qquad (4.4)$$

inner
beam

TE_{10}

helix

C

A

B

waveguide

ω

fast
space-
charge
wave

slow
space-
charge
wave

point C
degenerate
case

β

ω

n=-2 n=-1 n=0 n=+1

$\frac{2\pi}{L_H}$

point A

β

ω

TM_{01}
mode

n=-1

n=0

$\frac{2\pi}{L}$

point B
and within wave-
guide

β

$$\omega_n = \beta_n v_{01} + \frac{\omega_{p1}}{K_e} + (1 - \frac{v_{01}}{v_w})\, n\omega_w$$
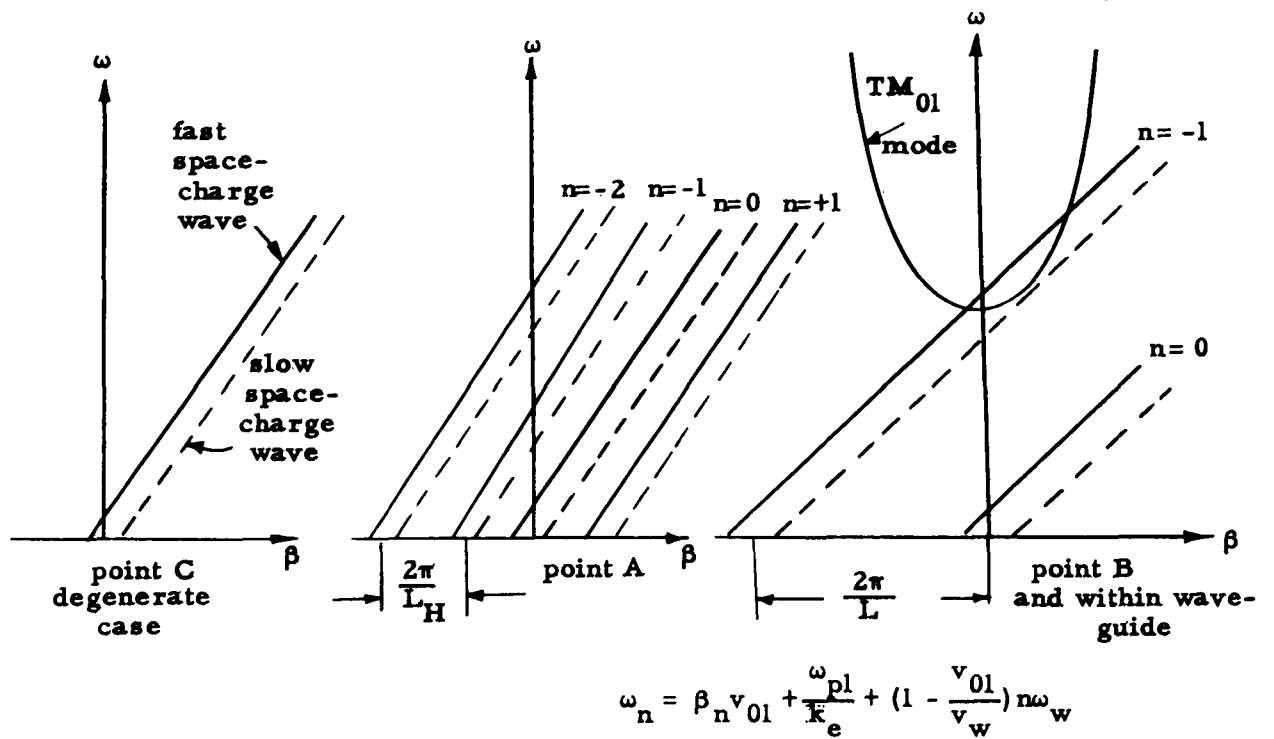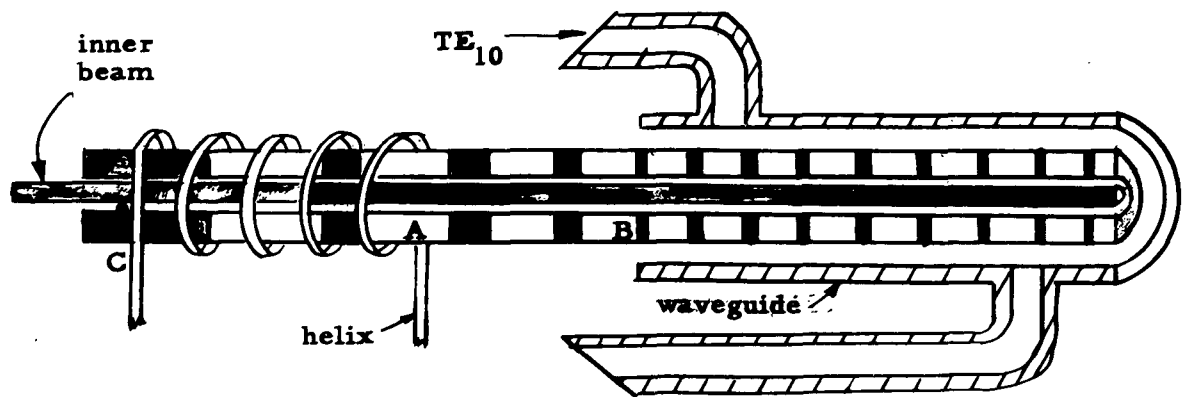
Fig. 10 Harmonics on inner beam

or
$$L \approx - \frac{\bar{v}_e n}{f} \qquad (4.4)$$

By combining Eqs. (4.4) and (4.3)

$$\frac{f}{f_H} = - \frac{\bar{v}_e n}{\bar{v}_{02}} \qquad (4.5)$$

where f is the signal frequency (about 24 Gc), f_H is. the frequency of the helix wave (about 2.4 Gc), $\bar{v}_e$ and $\bar{v}_{02}$ are the dc velocities of the inner and outer beams, respectively, within the cylindrical waveguide. Equation (4.5) is a fundamental equation because it explicitly shows how a high frequency signal f is related to the beam velocities and a much lower frequency f_H of a wave on the helix.

Note that for high-frequency operation Eq. (4.4) indicates that the periodicity L must be as small as possible.

It has been assumed that β_n is zero at the point of inter- action. For the interaction to occur where β_n is not zero the formula corresponding to (4.5) is

$$n f_H + \frac{\bar{v}_{02} f}{\bar{v}_e} = \frac{\bar{v}_{02} \beta_n}{2\pi} \qquad (4.6)$$

which reduces to Eq. (4.5) when β_n is zero. In the experimental tube the actual values would be only slightly different than those calculated by Eq. (4.5) so that the more exact Eq. (4.6) need not be used.

Equation (4.5) suggests that by letting, $\bar{v}_{02}$ approach zero the ratio $f/f_H \longrightarrow \infty$, which implies that a very-high-frequency signal could be amplified by a very low frequency on the helix. What prevents this state of events from being realized is the limiting perveance of the hollow beam within the waveguide, which limits both the values of $\bar{v}_{02}$ and ω_p that can be obtained.

4. Ideal bunching

The bunching of the hollow beam in the helix is non- linear. An approximate estimate of the amount of bunching may

- 31 -

be obtained by measuring the power gain of the helix wave by measuring the difference of the power of the electromagnetic wave as it enters and leaves the helix (taking into account circuit loss). This difference can be assumed to have been extracted from the hollow beam as the slow space-charge wave is excited and amplified. By measuring $\bar{v}_{0H}$ and f_H the period L_H is found by Eq. (4.2). From these measurements a general idea of the actual amplitude and period of the charge bunches on the hollow beam as it leaves the helix is obtained.

To calculate the amplitudes of the harmonics, it will be assumed that the beam is bunched in an optimum manner for obtaining harmonics, which is better bunching than the actual case discussed above. The idealized case is shown in Fig. 9. In the cylindrical waveguide a Fourier analysis of rectangular pulses of charge density gives

$$\rho = \rho_{02} + 2\rho_{02} \sum_{n=1}^{\infty} \frac{\sin \phi n \pi}{\phi n \pi} \sin \frac{2 \pi n z}{L} \qquad (4.7)$$

The term $\frac{\sin \phi n \pi}{\phi n \pi}$ will approach a maximum value of 1 as ϕ approaches zero, i.e., the width of the charge-density bunches decreases, leading to spikes of space-charge in the limit. This gives a maximum value for the terms in the series.

In the experimental tube, the hollow beam cannot be bunched in this manner, and even for efficient bunching $2\rho_{02} \cdot \frac{\sin \phi n \pi}{\phi n \pi} = \rho_m$ would probably lie between $\rho_{02}/2$ and $2\rho_{02}$. However, in Sec. IV. C the beam will be assumed to be a series of spikes of charge density with a corresponding value of $\rho_m = 2\rho_{02}$. Using this optimum value will give the largest possible value for the amplitudes of the harmonics on the inner beam, an upper bound which may not be exceeded.

The purpose of the tightly bunched hollow beam is to provide a periodic voltage on the axis of the tube. From the optimum value of ρ_m the magnitude of $\Delta \hat{V}_0$ can be calculated by first

calculating the E_z field on the axis, using $\nabla \cdot \bar{E} = \dfrac{\rho_m}{\epsilon}$, and

$\bar{E} \equiv |\bar{E}| \, e^{j(\omega t - \beta_b z)}$, where $\beta_b = \dfrac{2\pi}{L}$. If the electric fields were only in the z direction, $\bar{E}$ would be given by $\bar{E} = \dfrac{\rho_m}{-j\beta_b \epsilon}$. The transverse fields in the cylindrical guide are taken into account by using the plasma frequency reduction factor R.[18] E_z is given by

$$E_z = \frac{R^2 \rho_m}{-j\beta_b \epsilon} .$$

Since $E_z = \dfrac{\partial \, \Delta \hat{V}_0(z)}{\partial z} = j\beta_b \Delta \hat{V}_0$, therefore

$$\Delta \hat{V}_0 = \frac{R^2 \rho_m}{\beta_b^2 \epsilon} = \frac{R^2 \rho_m L^2}{4\pi^2 \epsilon} \tag{4.8}$$

This is the perturbation of the voltage on the axis due to the optimum bunched hollow beam, i. e. , the least upper bound of $\Delta \hat{V}_0$.

C. Amplitudes of the Harmonics for the Experimental Tube.

From Eq. (3.18) it follows that

$$\frac{|i_n|}{|i|} = J_n \left(\frac{L\Delta\beta}{2\pi} \right) \tag{4.9}$$

gives the normalized amplitude of the nth harmonic, i. e. , it gives the ratio of the amplitude of the nth harmonic to the sum of the amplitudes of all the harmonics. The argument of the Bessel function may be written as the product of two terms, one involving the inner beam and the other term involving the bunched beam:

$$\frac{L\Delta\beta}{2\pi} = \left(\frac{\beta_0}{4\pi \bar{V}_0} \right) (L \Delta \hat{V}_0) \tag{4.10}$$

Using Eq. (4.8), and the following auxiliary relations:

- 33 -

$$\omega_{q2}^2 = \frac{\eta \rho_m R^2}{\epsilon_0} \quad , \quad \beta_b = \frac{2\pi}{L} \quad , \quad \beta_0 \approx \frac{\omega}{\sqrt{2\eta \bar{V}_0}} \quad ,$$

Equation (4. 9) can be written as

$$J_n \left(\frac{L \Delta \beta}{2\pi} \right) = J_n \left[\left(\frac{\omega_{q2}}{\omega} \right)^2 \cdot \left(\frac{\beta_b}{\beta_0} \right)^3 \right] \tag{4.11}$$

This gives the argument for a beam bunched in the optimum manner described in Sec. IV. B.

The argument can now be calculated for typical values obtained from the experimental tube (assuming in addition a spike beam)

v_{02} = 200 volts	for beam 2
	O. D. = .320 mils
$\frac{\omega}{2\pi}$ = 24 Gc	I. D. = .120 mils
	R = .95
$\frac{\omega_H}{2\pi}$ = 2.4 Gc	K = 15 μ pervs.
	I_0 = 42.4 x 10^{-3} amp
	ω_{q2} = 1.46 Gc.

so that $\frac{L \Delta \beta}{2\pi} = .8 \times 10^{-4}$

n	$\dfrac{\|i_n\|}{\|i\|} = J_n \left(\dfrac{L \Delta \beta}{2\pi} \right)$
0	$\sim$ 1
1	$.4 \times 10^{-4}$
2	$.1 \times 10^{-8}$

This table shows that the amplitudes of the first and second harmonics are very small compared to the amplitude of the zeroth harmonic, even for the spike beam which gives an upper bound. In the limit when the argument goes to zero all the harmonics are zero except the zeroth one which has an amplitude of one, i.e., the space-time harmonics reduce to the ordinary fast

and slow space-charge wave as $\frac{L\Delta\beta}{2\pi} \to 0$. This is just about
the case for this tube, which is not at all desirable since for
appreciable interaction $\frac{L\Delta\beta}{2\pi}$ should be about 0.1, not $.4 \times 10^{-4}$.
The reason for this low value is that ω_{q2} is small compared to ω
and β_i has about the same magnitude as β (see Eq. (4.11)). The
low value of the plasma frequency ω_{q2} is due in turn to the limit-
ing perveance of the hollow beam in the waveguide.

Figure 11 shows the perveance of the hollow beam within
the waveguide as a function of the dc voltage of the beam. The
measured values of current and voltage indicate the perveance
has a peak value of 28.4 μ pervs which is the same as the limit-
ing perveance calculated from the dimensions of the hollow beam
and the waveguide.

Figure 12 shows that the cathode and collector current
rapidly fall off as the voltage is decreased from the value corre-
sponding to the limiting perveance. This indicates that due to
the depression of potential across the hollow beam inner electrons
are being returned to the cathode.

The major reason why the tube failed to operate is that a
dense beam is required, which was not physically obtainable since
only a limited amount of current at a given velocity may pass
through the cylindrical waveguide. The actual charge density of
the hollow beam in the experimental tube results in low values of
all the space-time harmonics except the zeroth harmonic. At-
tempts to increase the plasma frequency are not possible
in the experimental tube because the limiting perveance of the
beams within the waveguide may not be exceeded.

Unfortunately, the necessity of having an exceedingly dense
beam was not recognized until after the experimental tube was
built. The perveances were calculated from measured values of
voltages and currents, the outer beam shown to be bunched, and
there was transmission (no gain) of a 24 Gc RF signal through
the circuit. Using the measured values and the assumption of a

Fig. 11 Perveance of hollow beam within cylindrical waveguide
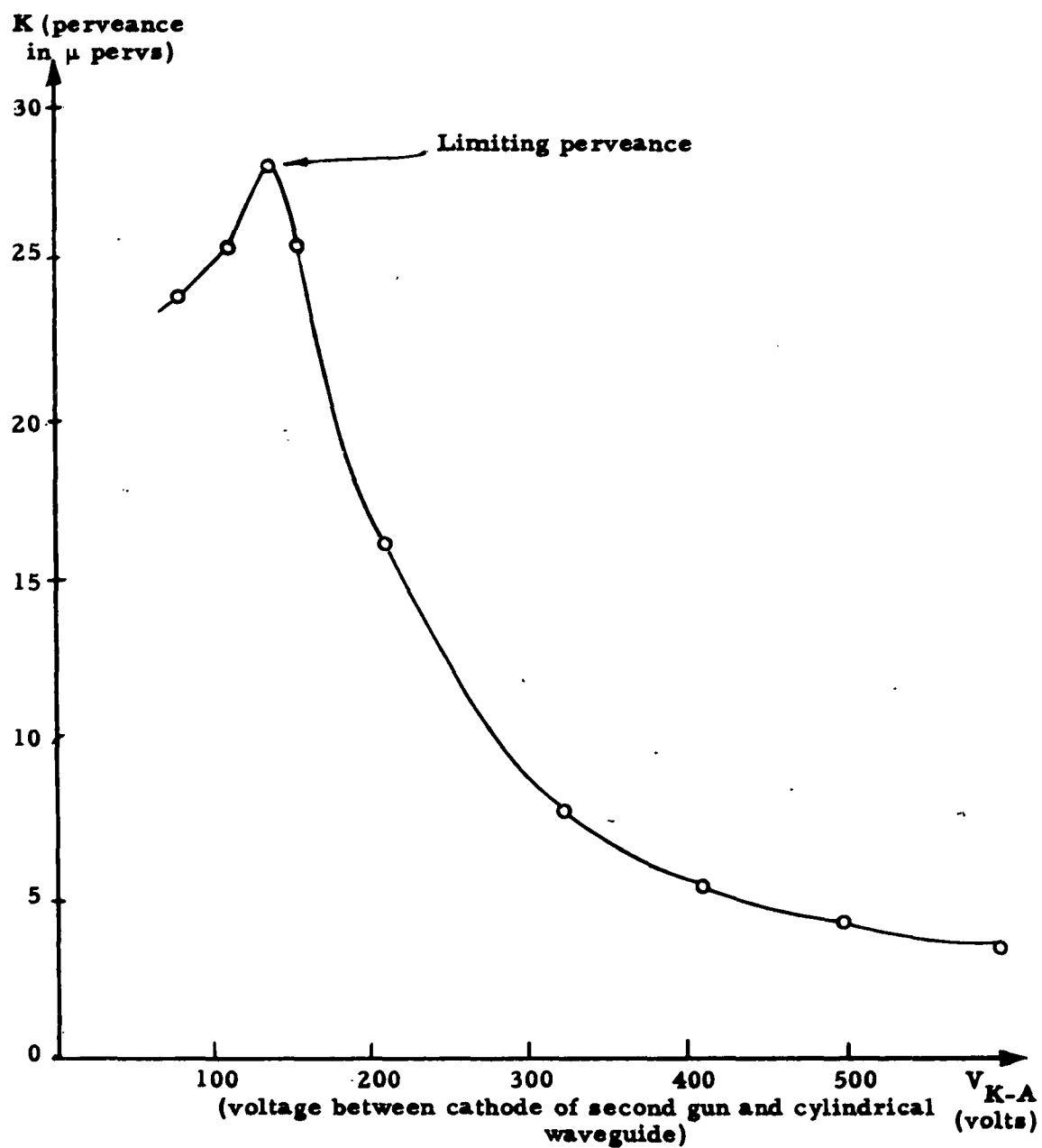
Note: K is perveance at entrance to waveguide.
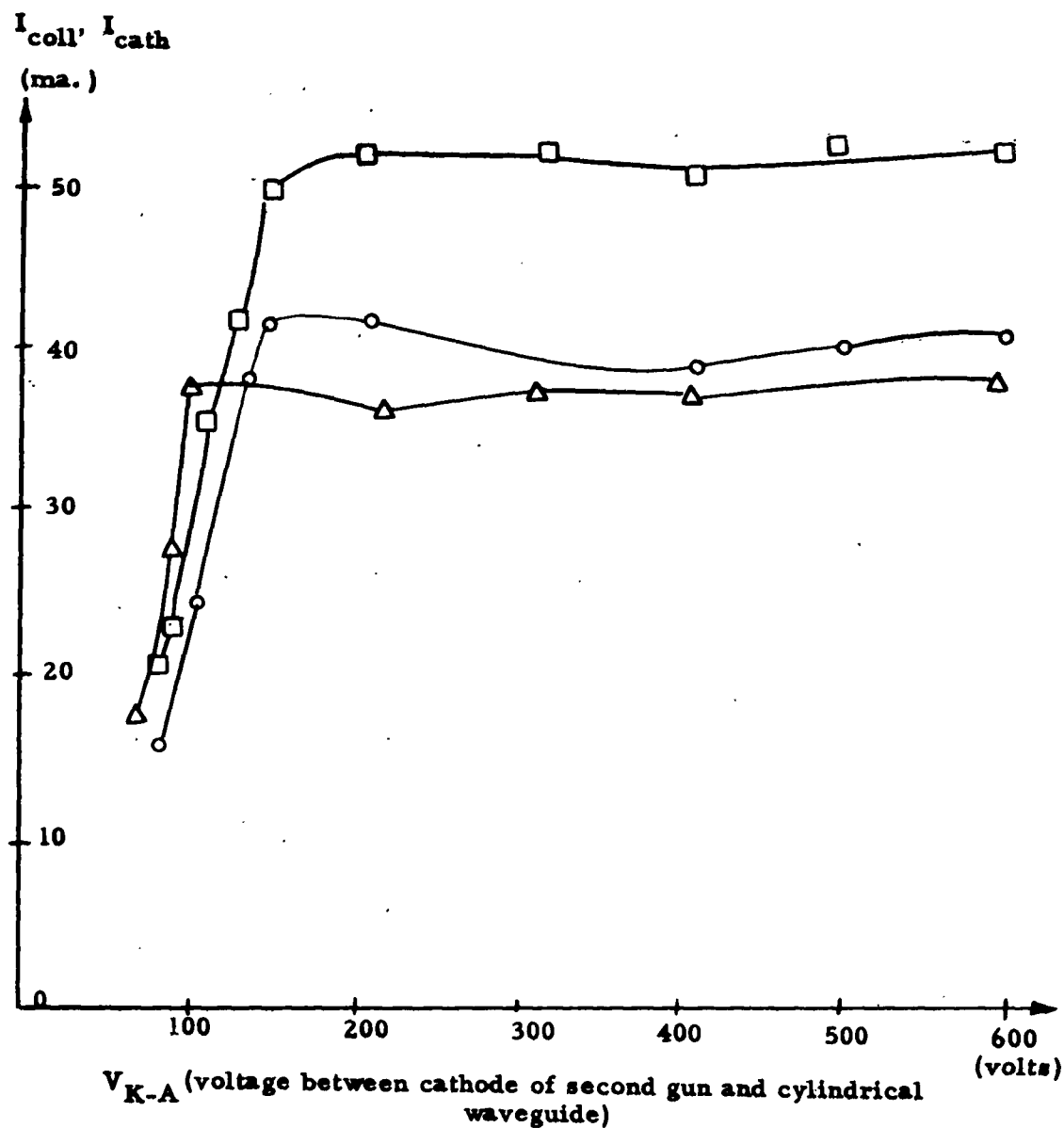
Voltage between cathode and anode of second gun held at 980 volts.

(from beam and waveguide dimensions calculated[18] limiting perveance is 28. 4 μ pervs.)

Fig. 12 Dependence of cathode and collector current
on voltage of hollow beam

- 37 -

"spike beam" an upper bound was then calculated by R. Carlile,
as shown on the previous pages.

The calculation of the amplitudes implicitly assumed
$\omega \gg \omega_{q2}$ as is the case for the experimental tube. If ω approaches
ω_{q2}, Eq. (3.18) is not valid as $\Delta\hat{V}_0 \approx \bar{V}_0$, and for an exact analysis
Mathieu functions are required. The use of Mathieu functions for
space harmonics[8,9] can be applied to the space-time harmonics
to determine the amplitudes of the space-time harmonics over an
extended range of signal frequencies.

D. Amplitudes of Space-Time Harmonics

In Sec. IV. C the amplitudes for the experimental tube
were calculated. In this section a general equation for the am-
plitudes of space-time harmonics is derived. The advantage of
this general equation is that the variation in the amplitudes as a
function of the signal frequency is explicitly stated. Using the
equation the amplitudes of space-time harmonics can be calcu-
lated for amplifiers designed to operate at millimeter wavelengths.

For a TM_{01} mode in a cylindrical waveguide the relation
between ω and β is the hyperbola

$$\beta = \pm \sqrt{\frac{\omega^2}{c^2} - k_c^2} \tag{4.12}$$

The relation between ω and β for space-time harmonics is
the straight line

$$\beta_n = \frac{\omega \pm \omega_p}{\bar{v}_e} + \frac{2\pi n}{L} \tag{4.13}$$

For each integer n there is a fast and a slow space-time
harmonic. The TM_{01} mode carries positive kinetic energy and
the slow space-time harmonic carries negative kinetic energy so
that amplification occurs when there is coupling between them.
Forward-wave coupling occurs when they have the same phase

velocity (the intersection of the straight line and the hyperbola) and the direction of the group velocity is the same. The group velocity is determined by the slope of the curves on the $\omega-\beta$ diagram and for amplification this corresponds to choosing the positive sign before the radical sign of Eq. (4.12). (It is also possible to couple between a space-time harmonic and the TM_{01} mode to get a BWO type interaction. The group velocity of the TM_{01} mode in this case is in the opposite direction of the harmonic and the negative sign before the radical sign of Eq. (4.12) would be chosen.)

Equating Eq. (4.12) and Eq. (4.13) a criteria for forward-wave interaction between the slow space-time harmonic and the TM_{01} mode is

$$\frac{\omega}{\bar{v}_e} + \left(\frac{2\pi n}{L} \pm \frac{\omega_p}{\bar{v}_e} \right) = + \sqrt{\frac{\omega^2}{c^2} - k_c^2}$$

or since $\beta_0 = (\omega \pm \omega_p)/\bar{v}_e$

$$\beta_0 + \frac{2\pi n}{L} = + \sqrt{\frac{\omega^2}{c^2} - k_c^2} \qquad (4.14)$$

Since n will be negative this equation can be rewritten

$$\frac{2\pi}{L} = \frac{1}{|n|} \left[\beta_0 - \sqrt{\frac{\omega^2}{c^2} - k_c^2} \right] \qquad (4.15)$$

The amplitudes of the space-time harmonics for a spike bunching beam were shown to have an upper bound

$$J_n \left[\left(\frac{\omega_{q2}}{\omega} \right)^2 \left(\frac{\beta_b}{\beta_0} \right)^3 \right]$$

Equation (4.11) can be simplified by using the added interaction condition derived by considering the relation between ω and β, that is, by substituting Eq. (4.15) in (4.11) and noting that $\beta_b = \frac{2\pi}{L}$ to get

- 39 -

$$J_n \left[(\frac{\omega_{q2}}{\omega})^2 \quad \left(\frac{\beta_0 - \sqrt{\frac{\omega^2}{c^2} - k_c^2}}{|n| \; \beta_0} \right)^3 \right] \qquad (4.16)$$

since

$$\frac{\omega^2}{c^2} > k_c^2 , \quad \beta_0 - \sqrt{\frac{\omega^2}{c^2} - k_c^2} < \beta_0$$

the amplitudes of the space-time harmonics have an upper bound given by

$$J_n \left[\frac{1}{|n|^3} \; \frac{\omega_{q2}^2}{\omega^2} \right] \qquad (4.17)$$

This equation shows that as the frequency of the signal is increased (for operation at millimeter wavelengths) the amplitude of the -1 space-time harmonic decreases as $\frac{1}{\omega^2}$.

For a given tube it can be seen from ω-β diagrams that the higher order harmonics intersect the hyperbola at higher frequencies so that one method of increasing the frequency of operation would be to use a higher order harmonic. Equation (4.17) indicates that the argument of the Bessel function is decreased by a factor of $1/|n|^3$ in addition to the term $1/\omega^2$ for this type of operation.

For BWO type interaction the amplitudes of the space-time harmonics are given by

$$J_n \left[(\frac{\omega_{q2}}{\omega})^2 \quad \left(\frac{\beta_0 + \sqrt{\frac{\omega^2}{c^2} - k_c^2}}{|n| \; \beta_0} \right)^3 \right] \qquad (4.18)$$

which has an upper bound

$$J_n \left[(\frac{\omega_{q2}}{\omega})^2 \quad \left(\frac{1 + \frac{V_e}{c}}{|n|} \right)^3 \right] \qquad (4.19)$$

For both forward wave and reverse wave interaction $\omega \gg \omega_{q2}$ and hence the amplitudes are too small for appreciable interaction at millimeter wavelengths.

V. CONCLUSIONS

This report presents a general analysis of space-time harmonics and the application of these harmonics to a specific electron-beam tube. This procedure allows a physical interpretation to be given to the equations for space-time harmonics, and points out fundamental limitations of the tube with two electron beams.

The electron-beam tube described in detail has the disadvantage that the amplitudes of the first and all higher order harmonics are too small for effective interaction by a factor of 10^4. The normalized amplitudes of the harmonics are given by Eq. (4.17).

The above analysis can be extended to other microwave amplifiers using space-time harmonics and provide the basis for evaluation of a large class of tubes. Section III gives a general discussion of space-time harmonics with respect to a single electron beam and a structure upon which three restrictions are placed. Intuitively the requirements placed on the structure imply that it gives a moving periodic voltage on the axis of the tube. Specific examples, such as apertured disks, serve to illustrate various possibilities but the analysis does not rely on any specific structure. Hence, radically different means of providing a periodic voltage on the axis can be investigated.

The general analysis of Section III leads to the fundamental equation (3.18) which explicitly states the space-time harmonic current in the beam. This equation shows that the current variation consists of an infinite number of space harmonics whose amplitudes are given by various-order Bessel functions.

A second necessary condition is that one of the harmonics should have the proper ω-β characteristics for interaction with an electromagnetic wave. An ω-β diagram for the harmonics can be constructed from Eq. (3.18) and by superposition of the ω-β diagram of the circuit for the electromagnetic wave a method is readily obtained for investigating possible regions of interaction.

These two fundamental conditions are interrelated. By specifying the region of interaction of the harmonics the dc velocity and periodicity of the beam is constrained, and these factors enter into the determination of the amplitudes. A step-by-step procedure for evaluating any proposed tube is outlined below:

(1) Construct an ω-β diagram of the harmonics and the circuit of the electromagnetic wave. Figure 3 is an example of such a diagram for the case where the circuit is a cylindrical waveguide. This circuit has the advantage of simplicity and is readily usable for millimeter waves. It is essential that one harmonic can interact with the wave. Equation (4.6) explicitly states this condition.

(2) Calculate the magnitude of the periodic voltage on the axis of the tube due to the structure, i.e., calculate $\Delta \hat{V}_0$. This is dependent upon the particular structure chosen. (For example, a possible structure is a hollow bunched beam which has a value $\Delta \hat{V}_0$ given by Eq. (4.8).)

(3) Calculate the amplitudes of the harmonics by combining steps (1) and (2). If the amplitude of the harmonic of interest is within the range 0.01 to 1.0, then the proposed tube will be satisfactory. (For the dual beam tube in a cylindrical waveguide the amplitudes are given by Eq. (4.10).)

The procedure outlined above is followed in Sec. IV for the idealized two-beam tube. To maximize the normalized current ratio as given by Eq. (4.10), the plasma frequency ω_{q2} should be as large as possible, but is limited by the maximum perveance

of the beams within the cylindrical waveguide. This maximum available value of ω_{q2} appears to be a fundamental limitation on dual beam tubes.

Finally, as the frequency of the signal is increased (for operation at millimeter wavelengths) the amplitude of the -1 harmonic decreases as $1/\omega^2$.

In general the amplitude of the harmonics for the idealized two-beam tube decrease as the frequency increases and this fundamental limitation, together with the maximum obtainable ω_{q2}, indicate that this type of dual-beam tube is not practical for wideband millimeter wavelength operation.

APPENDIX A: HOLLOW BEAM AS A PERIODIC STRUCTURE

This appendix covers a mode of operation for the experimental tube described in Secs. I-III which is unrelated to the method of amplification previously discussed. It is surprising that a tube designed to operate in one mode may also operate in an entirely different mode. However, owing to the small value of the amplitudes of the partial waves for the experimental tube, operation in the new mode is unsatisfactory, as shall be shown more clearly below. In Secs. I-III the two beams interacted to yield conditions for harmonics on the inner beam. The tube was designed to utilize this interaction. In this appendix the interaction between beams will be completely ignored. Instead, the hollow bunched beam is considered to be a periodic structure which interacts with the electromagnetic wave. The distinction between the two modes of operation is shown in Fig. 13.

The key point is to consider the hollow bunched beam as a periodic structure. All the properties of periodic structures such as stopbands and passbands can be applied to the periodic bunched beam. There is only one difference between the bunched beam and the periodic structures such as disk-loaded waveguides

Method I
(used in Secs. I-III)

(1) Consider the hollow outer beam to interact with inner beam to give a set of space-time harmonics on the inner beam.
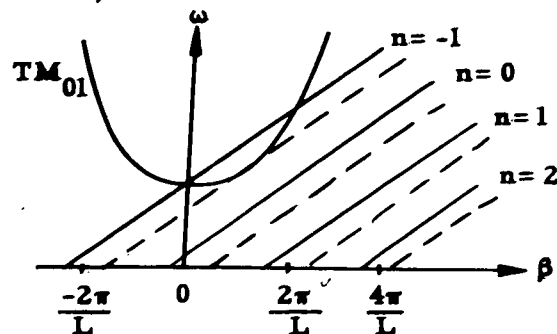
(2) Then consider interaction between one harmonic and TM_{01} mode in the wave-guide.

TM_{01}

n= -1
n= 0
n= 1
n= 2

ω

β

$\frac{-2\pi}{L}$ 0 $\frac{2\pi}{L}$ $\frac{4\pi}{L}$

$$i = \sum_{n=-\infty}^{\infty} |i| \, J_n(\frac{L\Delta\beta}{2\pi}) \, e^{j[\omega t-(\beta_0+\frac{2\pi n}{L})z]}$$

Method II
(Used in Appendix)

(1) Consider hollow outer beam to interact with the TM_{01} mode to give a set of partial electromagnetic waves.

(2) Then consider the interaction between one partial wave and the slow space-charge wave on the inner electron beam.

ω

n= 0   n= 1   n= 2

slow space-charge wave

β

$-2\pi/L$ 0 $2\pi/L$ $4\pi/L$
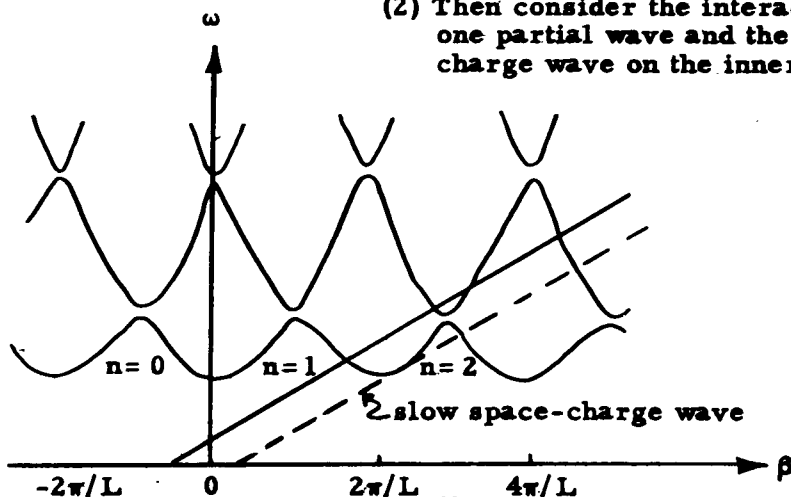
$$E = \sum_{n=-\infty}^{\infty} |E| \, J_n(\frac{L\Delta\beta}{4\pi\epsilon_0}) \, e^{j[\omega t - \beta_n(z)z]}$$

$$\beta_n(z) = (\omega\sqrt{\mu\epsilon_0} + \frac{2\pi n}{L})$$

Fig. 13 Comparisons of methods used in Secs. I-III and
Appendix

and helices of particular interest—the electron beam is moving with
respect to the laboratory frame of reference. This leads only to
a minor change for the conditions present in the experimental
tube.

As in all periodic structures, an electromagnetic wave
will consist of a set of spatial harmonics as it passes through
the periodic structure. Since it is impossible to satisfy the
boundary conditions with only one of these harmonics, all of them
are excited if a wave travels down the guide. This makes these
spatial harmonics similar to the space-time harmonics con-
sidered in Secs. I-III but different from modes in ordinary smooth
waveguides which may exist singly, since each TE or TM mode
satisfies the boundary conditions. The purpose of this appendix is
to find an interaction impedance K_n. To this end several simpli-
fying assumptions are made. The mathematics is very similar to
that of Secs. I-III, but the underlying physical behavior is dif-
ferent. Once K_n is found the analysis is parallel to that used by
Pierce.[17]

The beam is replaced by a dielectric which has a sinusoidal
variation, shown in Fig. 14. Assuming an electromagnetic wave
propagates down the waveguide with a time dependence

$$e^{j\omega t} \tag{A.1}$$

from Maxwell's equations and the periodic $\epsilon(z)$ given by

$$\epsilon(z) = \epsilon_\ell + \Delta\epsilon_\ell \sin\beta_b z \qquad (\Delta\epsilon_\ell \ll \epsilon_\ell , \ \beta_b = \frac{2\pi}{L}) \tag{A.2}$$

one gets the pair of equations

$$\nabla^2 H = -\omega^2 \mu\epsilon(z) H - j\omega\beta_b \Delta\epsilon_\ell (\cos\beta_b z)\bar{a}_z \times E \tag{A.3}$$

$$\nabla^2 E = -\omega^2 \mu\epsilon(z) E - \frac{\Delta\epsilon_\ell \beta_b(\cos\beta_b z)}{\epsilon(z)} \nabla E_z + \frac{\Delta\epsilon_\ell \beta_b^2(\sin\beta_b z)}{\epsilon} E_z\bar{a}_z \tag{A.4}$$
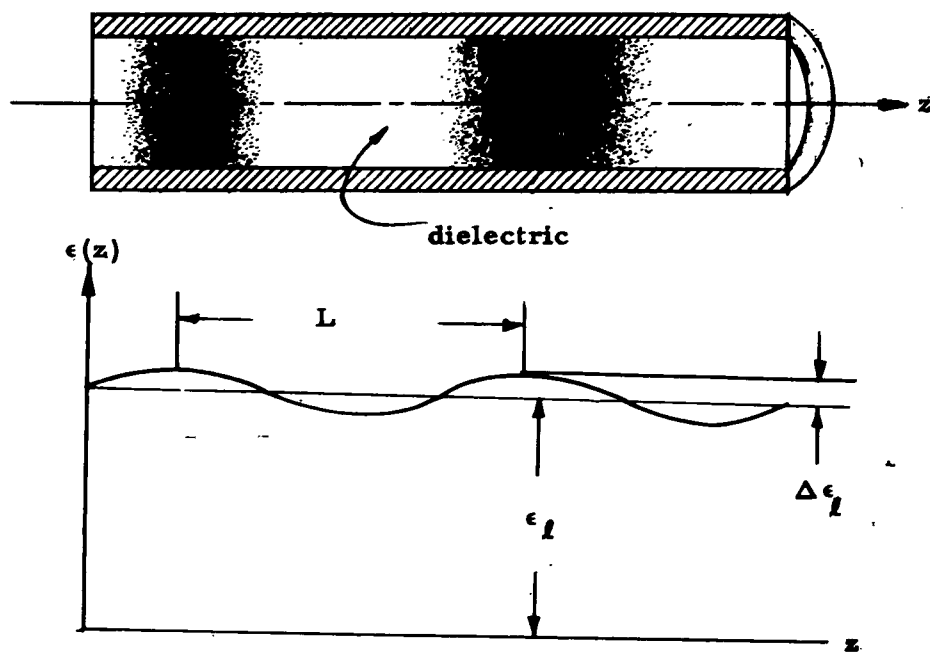
$$\epsilon(z) = \epsilon_l + \Delta\epsilon_l \ \sin\frac{2\pi z}{L}$$

$$\Delta\epsilon_l < \epsilon_l$$

Fig. 14 Model used in method II of Fig. 13, where beam is replaced by a dielectric

Note that if $\Delta\epsilon_\ell = 0$ the above two equations reduce to the ordinary wave equations

$$\nabla^2 \mathbf{H} = -\omega^2 \mu\epsilon_\ell \mathbf{H} \qquad \nabla^2 \mathbf{E} = -\omega^2 \mu\epsilon_\ell \mathbf{E} \qquad (A.5)$$

The component of the $\mathbf{E}$ field which will interact with the slow space-charge wave on the inner beam is the E_z component, which can be written as

$$\nabla^2 E_z = \left(\frac{\Delta\epsilon_\ell \, \beta_b^2 \sin\beta_b z}{\epsilon_\ell} - \omega^2 \mu\,\epsilon(z) \right) E_z - \frac{\Delta\epsilon_\ell \, \beta_b (\cos\beta_b z)}{\epsilon(z)} \frac{\partial E_z}{\partial z}$$

$$(A.6)$$

The first assumption is that $\Delta\epsilon_\ell < \epsilon_\ell$ which implies that the effect of the periodicity is small.

If $\epsilon(z) = \epsilon_\ell$, i.e., if there were no variation in z, the solution would be

$$E_z = E_z(x, y)\, e^{j(\omega t - \beta z)} \qquad (A.7)$$

$(\beta = \omega\sqrt{\mu\epsilon_\ell}\,)$

Since there is in fact variation in z, $\epsilon(z) = \epsilon_\ell \, \Delta\epsilon_\ell \, \sin\beta_b z$, the actual value of E_z will be different than Eq. (A.7), but the equation can be considered a first order approximation. Therefore

$$\frac{\partial E_z}{\partial z} \approx -j\beta E_z \qquad (A.8)$$

Assuming $\beta_b > \beta$

$$\nabla^2 E_z \approx -\beta^2 \left[1 - \frac{\beta_b^2}{\beta^2} \frac{\Delta\epsilon_\ell}{\epsilon_\ell} (\sin\beta_b z) \right] E_z \qquad (A.9)$$

so that

$$E_z = E_z(x, y) e^{j[\omega t - \int_0^z \beta\sqrt{1 - \frac{\beta_b^2 \Delta\epsilon_\ell}{\beta^2 \epsilon_\ell}(\sin\beta_b z)}\; dz]}$$

$$(A.10)$$

- 47 -

Equation (A. 10) is a second order approximation of E_z. Assuming

$$\frac{\beta_b^2 \Delta \epsilon_\ell}{\beta^2 \epsilon_\ell} < 1 \qquad (A.11)$$

one can rewrite Eq. (A. 10)

$$E_z = E_z(x, y)\ e^{j[\omega t - \int_0^z \beta(1 - \frac{\beta_b^2 \Delta \epsilon_\ell}{2\beta^2 \epsilon_\ell} \sin \beta_b z)\ dz\ ]} \qquad (A. 12)$$

$$E_z = E_z(x, y)\ e^{j[\omega t - (\beta z + \frac{\beta_b \Delta \epsilon_\ell}{2\beta \epsilon_\ell} \cos \beta_b z)]} \qquad (A. 13)$$

$$E_z = \sum_{n=-\infty}^{\infty} |E_z|\ J_n(\frac{\beta_b \Delta \epsilon_\ell}{2\beta \epsilon_\ell})\ e^{j[\omega t - \beta z + \beta_b n z]} \qquad (A.14)$$

This gives the second-order approximation for the fields for the waveguide filled with a periodic dielectric. How the dielectric corresponds to the hollow bunched beam remains to be shown.

One can choose a frame of reference X' moving with the bunched electron beam. The equations developed for E so far have tacitly assumed that the laboratory frame of reference (a stationary frame of reference X) is used. But all these equations may be transformed to the moving frame of reference by transformations similar to those in Sec. II. B. However, Eqs. (A. 1) to (A. 14) appear essentially the same in the moving frame of reference X', since the Doppler shift and relativistic corrections of the electromagnetic wave are small in the experimental tube.

The beam appears as a plasma in X' and for an infinite magnetic field this plasma may be considered a dielectric and will correspond to the permittivity in the previous equations. The transformation from X to X' does not materially influence the electromagnetic wave but permits one to replace the beam by a

plasma. The dielectric constant corresponding to a plasma is

$$\epsilon_L = \epsilon_0 (1 - \frac{\omega_{q2}^2}{\omega^2}) \quad \text{(longitudinal component)}$$

(A.15)

$$\epsilon_T = \epsilon_0 \quad \text{(transverse component)}$$

Up to this point no distinction has been made between longitudinal and transverse components of the permittivity, as the permittivity was tacitly assumed to be a scalar periodic in z. In the experimental tube the frequency ω is sufficiently greater than the plasma frequency so that $\omega_{q2}/\omega \ll 1$ and the preceding equations are essentially correct. More explicitly, one assumes an infinite magnetic field and the relation

$$\epsilon_\ell = \epsilon_L = \epsilon_0$$

(A.16)

With no beam present the permittivity of the empty guide is ϵ_0. With an unbunched beam present in the waveguide the permittivity is given by Eq. (A.15). For a bunched beam as shown in Fig. 16 $\Delta \epsilon_\ell \approx 1 (\omega_{q2}^2/\omega^2) \epsilon_0$. This states, in effect, how well the hollow beam is bunched.

Replacing the beam by an equivalent dielectric, Eq. (A.14) for the set of partial electromagnetic waves becomes

$$E_z = \sum_{n=-\infty}^{\infty} |E_z| J_n (\frac{\beta_b \omega_{q2}^2}{2\beta\omega^2}) e^{j[\omega t - \beta z + \beta_b nz]}$$

(A.17)

The interaction impedance is

$$K_n = \frac{E_{nz}^2}{2\beta_n^2 P}$$

(A.18)

Note that

$$\frac{|E_{nz}|}{|E_z|} = J_n (\frac{\omega_{q2}^2 \beta_b}{2\omega^3 \sqrt{\mu \epsilon_\ell}})$$

(A.19)

For the experimental tube (using values on page 3¦4)

n	$\dfrac{\lvert E_{nz} \rvert}{\lvert E_z \rvert}$
0	~ 1
1	3×10^{-4}
2	1.1×10^{-8}

These small values of $\lvert E_{nz} \rvert / \lvert E_z \rvert$ indicate low values of the inter-action impedance and it is not surprising that no gain was observed in the experimental tube.

REFERENCES

1. Ramo, S., "Space Charge and Field Waves in an Electron Beam," Phys. Rev., Vol. 56 (1939), pp. 276-283.

2. Hahn, W. C., "Small-Signal Theory of Velocity-Modulated Electron Beams," Gen. Elec. Rev., Vol. 42 (1939), pp. 258027O.

3. Müller, R., "Teilwellen in Elektronenströmugen," Archiv. d. elektr. Uebertrag, Vol. 10 (1956), pp. 505-511.

4. Mueller, W., "Direct-Current and Wave Behavior of Electrostatically Focused Electron Beams," Doctoral Thesis, Univ. of California, Berkeley.

5. Bloom, S., Peter, R. W., and Ruetz, J. A., "Space-Charge Wave Amplification along an Electron Beam by Periodic Change of the Beam Impedance," RCA Review, Vol. 15 (1954), pp. 113-120.

6. Bernashevskii, G. A., "Raumharmonische des Elektronenstrahles," Radiotechnika u. Elektronika, No. 1 (1957), pp. 124-125.

7. Mueller, W. and Staprans, A., "Propagation in Periodic Electron Beams," Sixteenth Annual Electron Tube Research Conference, Quebec, Canada (June 27, 1958).

8. Staprans, A., "A Study of Space-Charge-Wave Propagation in Periodic Electron Beams," ERL Report, Univ. of California, Series No. 60, Issue No. 225, 1959.

9. Mueller, W., "Propagation in Periodic Electron Beams," J. Appl. Phys., Vol. 32 (1961), pp. 1349-1360.

10. Müller, R., "Space and Time Harmonics on Electron Beams," Symposium on Electronic Waveguides, New York; Polytechnic Institute of Brooklyn, Vol. 8, 1958.

11. Stratton, J. A., Electromagnetic Theory, New York; McGraw-Hill Book Co., 1941.

12. van der Pol, B., "The Fundamental Principles of Frequency
     Modulation," JIEE, Vol. 93, Part III (1956), pp. 153-158.

13. Chu, L.J., "A Kinetic Power Theorem," IRE Conference on
     Electron Devices, New Hampshire; Durham, 1951.

14. Gould, R.W., "A Coupled Mode Description of the Backward-
     Wave Oscillation and the Kompfner Dip Condition,"
     Trans. IRE, ED-2, No. 4 (1955).

15. Heffner, H., "A Coupled Mode Description of Beam-Type Ampli-
     fiers," Proc. IRE, Vol. 43 (1955), pp. 210-217.

16. Pierce, J.R., "The Wave Picture of Microwave Tubes," Bell
     Syst. Tech. J., Vol. 33 (1954), pp. 1343-1372.

17. Pierce, J.R., Traveling-Wave Tubes, New York: D. Van Nostrand
     Co., 1950.

18. Branch, G.M. and Mihran, T.G., "Plasma Frequency Reduction
     Factors in Electron Beams," Trans. IRE, ED-2, No. 2
     (1955).

Aeronautical Systems Division, Dir/Avionics, Electronic Technology
Lab, Wright-Patterson AFB, Ohio.
Rpt nr ASD-TDR-63-527. LIMITATIONS OF SPACE-TIME HARMON-
ICS FOR MICROWAVE AMPLIFICATION
Interim report, Mar 62, 52 p. incl. illus., tables, 18 refs.

Unclassified Report

The possibility of gain utilizing the interaction between an electro-
magnetic wave in a smooth wave guide and a space-time harmonic
of the slow space-charge wave has been proposed as a method of
millimeter-wave amplification. A model is proposed here which
satisfies the conditions necessary for the existence of space-time
harmonics. This model is an idealization of a tube having two
electron beams where the periodic variation of the dc parameters
of the inner beam is provided by a bunched hollow outer beam.
Since the periodic variation of the inner beam results from the
moving electric field of the bunched beam rather than stationary
electric or magnetic fields, the device illustrates an application
of space-time harmonics rather than space harmonics and intro-
duces a new method of providing the required periodic variations.
A small signal analysis of the model leads to vanishingly small
expressions for the amplitudes of the n = 1, 2,...space-time
harmonics, and hence to the conclusion that for the model con-
sidered amplification over a wide band of frequencies is not
practical.

1. Electromagnetic Waves
2. Electronic Beams
3. Microwave Tubes
4. AFSC Project No. 4150
   Task No. 415001
II. Contract AF 33(657)-764
   BPSN: 2n60-4150
III. Univ. of California,
   Berkeley, Calif.
IV. I.E. Everhart
   J. Horowitz
V. ERL Series No. 60
   Issue No. 440
VI. Avail fr OTS
VII. In ASTIA collection